INVESTIGATING THE DETERIORATION OF BASEMENT WALLS MADE OF CONCRETE IN CT

by

Kay Wille[1] and Rui Zhong[2]

[1] Associate Professor and PI of the project, [2] Postdoctoral Researcher

August, 31st 2016

Department of Civil and Environmental Engineering

Advanced Cementitious Materials and Composites (ACMC) Laboratory

University of Connecticut

Storrs, CT 06269

This report was produced for the

Attorney General of the State of Connecticut.

TABLE OF CONTENTS

LIST OF FIGURES

LIST OF TABLES

1. INTRODUCTION

1.1 BACKGROUND

On August 6, 2015, the Attorney General and Commissioner of Consumer Protection of the State of Connecticut were asked by Governor Dannel P. Malloy to investigate whether Connecticut's consumer protection laws were violated in connection with the construction of homes in Eastern Connecticut experiencing deterioration of their concrete foundations. Pursuant to that investigation, the Attorney General and Commissioner of Consumer Protection retained the authors to assist in understanding the likely causes of the deterioration.

Early deterioration of concrete home foundations located in an area of Eastern Connecticut has caused alarm to homeowners, and thus to state agencies, affected communities and others. Many homeowners face significant financial and other burdens relating to the deterioration of their concrete home foundations. In some cases, the deterioration is severe. In light of these circumstances, it is of great public interest, and academic value, to understand what may have caused the deterioration.

Through site inspections and the rigorous testing and analysis of samples of deteriorating home foundation concrete and concrete aggregate, this report seeks to bridge an existing knowledge gap concerning why some home foundations in Eastern Connecticut are prematurely deteriorating. While the potential methods of repair, as well as the full scope of the problems in terms of the number of potentially affected structures, are beyond the scope of the Governor's referral and of this report, the information contained herein represents a significant advancement of the scientific understanding of the basic causal factors underlying this problem.

1.2 OBJECTIVE

The objective of the proposed research is to investigate the deterioration of concrete foundation in an area of Eastern Connecticut and thereby gain a better understanding of what could have caused

the premature deterioration. Special emphasis will be placed on answering the following questions:

1) What are the symptoms and characteristics of the deterioration?
2) What is the strength loss of the material?
3) Is the concrete mixture (i.e., choice of aggregate and cement, mixture design) linked to the deterioration?
4) Did environmental conditions, including soil conditions, impact the deterioration?
5) Was knowledge about the deterioration potential of concrete constituents available at the time that the affected concrete was produced and the home foundations were installed?

1.3 EXECUTIVE SUMMARY OF RESEARCH APPROACH

Based on the investigators' experience in concrete technology, material design and characterization, the following research steps were undertaken:

1) SITE VISITS AND SAMPLING: Selecting houses for potential inspection and investigation based on their construction date, degree of deterioration and geographical distribution. Documenting the symptoms of deterioration, such as crack pattern, crack opening, discoloring and spatial distribution of deposition at the vicinity of cracking surface. Collecting material samples at the cracking surface and drilling core samples out of concrete foundation walls and slabs both at damaged and intact areas.
2) CONCRETE STRENGTH: Testing of the residual compressive strength and analyzing the failure pattern of deteriorated concrete.
3) MINERAL CHARACTERIZATION: Emphasis of this characterization is placed on the detection of iron sulfide such as pyrite (FeS_2) and pyrrhotite ($Fe_{1-x}S$ (x=0 to 0.125)). Aggregates of the obtained core samples and aggregates of the supplying quarry were examined and in their mineral phases analyzed. Additionally, the mineral phases of the depositions at the vicinity of the cracking surface were characterized. X-ray diffraction

(XRD) and X-ray fluorescence (XRF) technologies were used for analysis purpose. Supplementary scanning electron microscopy (SEM) coupled with energy dispersive X-ray (EDX) test was also conducted for the investigation of quarry aggregate to overcome the limits of the XRD technology and confirm the XRF results.

4) INVESTIGATION OF SULFATE BASED REACTION PRODUCTS: Emphasis was placed on investigating the micro structure of the interfacial transition zone (ITZ) between aggregate and cement matrix, as well as the matrix itself, using SEM coupled with EDX. Point analysis was conducted to confirm the existence of minerals such as ettringite and thaumasite and their delayed formation. Mapping analysis was used to validate the oxidization of the pyrrhotite-bearing aggregates.

Fig. 1.1 schematically summarizes the research approach, in which visible macroscopic properties are linked to scientific microstructural parameters.

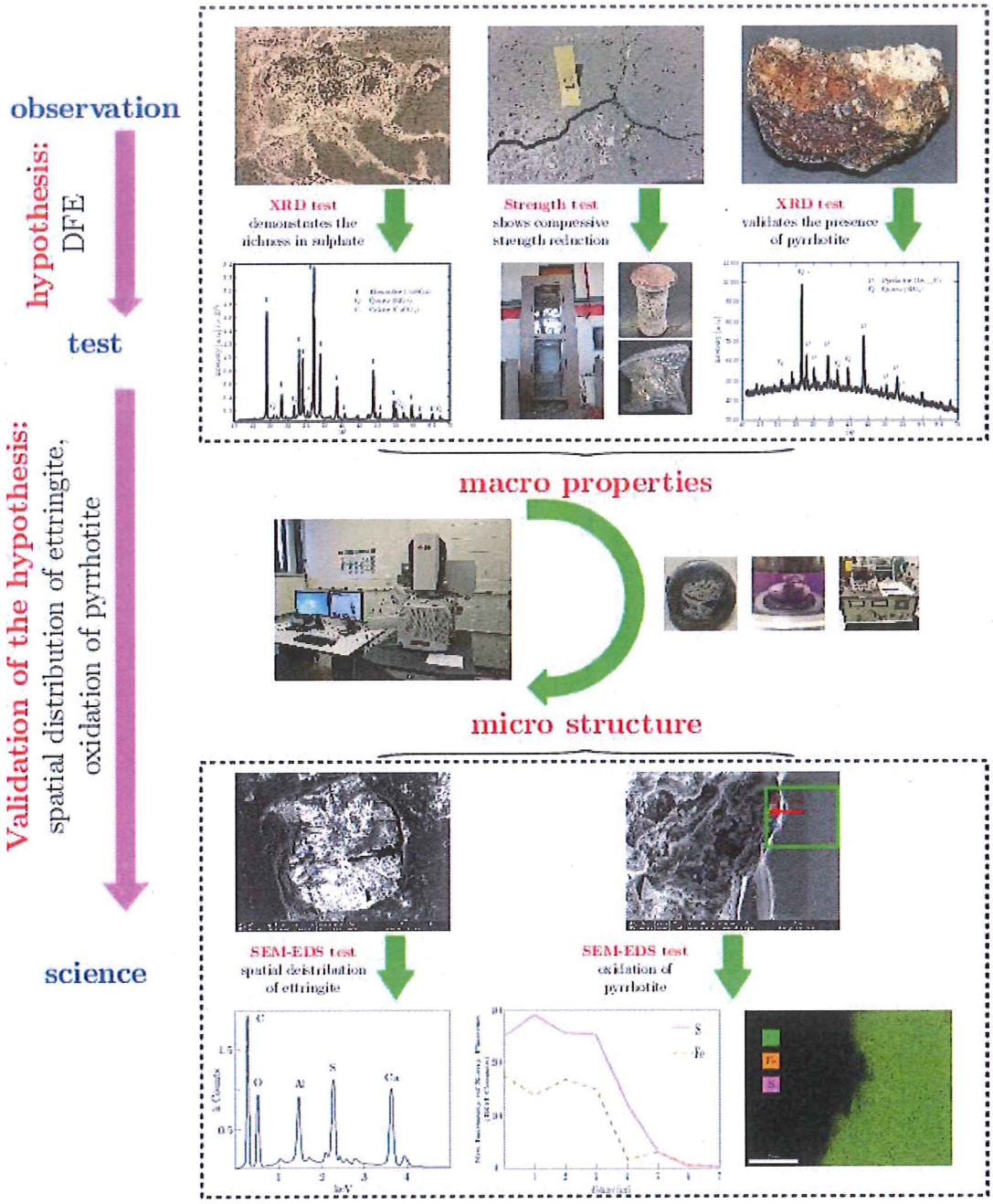

Fig. 1.1 Research Approach

Based on visual inspection typical deterioration symptoms can be identified, such as map cracking, whitish formation of minerals at the vicinity of the cracking surface and reddish - brownish discoloring. After experimental testing and microstructural investigation the results were analyzed and correlated to the deterioration symptoms of the visual inspection. Based on the

obtained results the investigators conclude that the oxidation of pyrrhotite-containing aggregates and the associated secondary formation of expansive minerals are the primary cause of the early deterioration of these concrete wall foundations. It is worth noting that the presence of pyrrhotite-containing aggregates alone does not necessarily lead to its oxidation and concrete deterioration.

1.4 OUTLINE OF REPORT

This final report is divided into seven chapters. The first chapter is an introduction to the research project, its objectives and research approach. Chapter two provides background information such as deterioration of concrete derived from sulfate attack and secondary mineral formation, historical investigation and existing standards related to concrete deterioration induced by sulfide-bearing aggregate. Chapter three presents detailed onsite survey results of candidate houses. Chapter four provides information regarding the compressive strength investigation. Chapters five and six cover mineralogical assessment of the quarry aggregate, aggregate from the crushed core samples and mineral formations at the vicinity of cracking surface. Chapter seven presents the microstructural investigation of deteriorated concrete. Chapter eight summarizes the principal findings and conclusions.

2. BACKGROUND INFORMATION

Based on the reported typical symptoms of deterioration, it is hypothesized that the damage is caused by the oxidation of sulfide-bearing aggregate that leads to expansive secondary mineral formation such as iron hydroxide, gypsum, ettringite, and thaumasite. Therefore research emphasis is placed on the mechanisms of such deterioration.

2.1 SULFATE ATTACK

2.1.1 INVESTIGATION OF THE DETERIORATION OF CONCRETE STRUCTURE DERIVED FROM SULFATE ATTACK

Normal Portland cement concrete is known to undergo an increase in volume and subsequently cracking under long exposure to sulfate enriched solutions. This phenomenon is called sulfate attack. It results from the chemical reaction between the products of cement hydration and the sulfates. The problem of sulfate attack raised concerns around 1890 due to failures on a railway in southern France. In 1900 and 1902 further problems due to sulfate attack by gypsum, magnesium and sodium sulfate were found in tunnels in France and in structures in southern Algeria [1]. Lea and Desch point out that clays and soils are found containing considerable amount of mineral sulfates in many parts of Great Britain and in many extensive regions outside of England [2]. Sulfate-bearing soils are also present in France and other parts of Europe, as well as across large areas of the United States and Canada. The problems associated with sulfate attack are therefore of widespread interest across North America and Europe.

In the early 1990s, the National Bureau of Standards (NBS), the U.S. Department of Agriculture (USDA) and the Portland Cement Association (PCA) in the United States, as well as the Engineering Institute and the National Research Council in Canada conducted extensive research on the deterioration of concrete due to sulfate attack. The field and laboratory studies conducted and conclusions drawn by these organizations are reviewed in the following sections.

The NBS initiated a study in 1910 to investigate the resistance of concrete exposed to seawater [3]. However, this program eventually developed into a study of the deterioration of concrete by sulfate-containing water. Hollow mortar cylinders with varying cement-sand ratios were filled with salt solutions in the preliminary study. One conclusion from this study was:

Portland cement mortar or concrete if porous enough can be disintegrated by the mechanical forces exerted by the crystallization of almost any salt in its pores, if a sufficient amount of it is permitted to accumulate and a rapid formation of crystals is brought about by drying. Porous stone, brick and other structural materials are disintegrated in the same manner. Therefore, in alkali regions where a concentration of salts is possible, a dense nonporous surface is essential.

This preliminary study was followed by a cooperative investigation in 1914 involving the USDA, U.S. Bureau of Reclamation and the American Portland Cement Manufactures Association [4]. Drain tile made with Portland cement was exposed to alkali soils in South Dakota, Colorado, Washington, New Mexico, Arizona, Minnesota, Missouri and Iowa. The experiments were extended to include concrete blocks containing reinforcing steel. Progress reports on this work were prepared in 1917, 1922 and 1926 [4-6]. Some of the conclusions were as follows:

1) *Disintegration may be manifested in sulfate water by physical disruption by expansion resulting from crystallization of salts in pores, but it is primarily due to chemical reaction between salts in solution and the constituents in cement.*
2) *The use of tile in soils containing alkali salts of the sulfate type in considerable quantities is hazardous, since some specimens of the best quality have been disintegrated during an exposure of less than 6 years.*

In the spring of 1919, a number of failures of drain tile in the ground in southwestern Minnesota drew attention of the USDA. Consequently, a laboratory at the University of Minnesota was established for the purpose of investigating the issues associated with the deterioration of concrete. An extensive study was conducted under the direction of Dalton G. Miller [7-9]. The

chemical analysis from the U.S. Bureau of Soils on 1062 water samples and 150 soil samples revealed that the failures were closely associated with the presence of sodium and magnesium sulfates. The performance of specimens made by 122 cements stored in tap water, Medicine Lake and solutions of Na_2SO_4 and $MgSO_4$ were evaluated. Based on the strength ratio between the samples stored in Medicine Lake and tap water and the number of months required to reach an expansion for 0.01%, Miller and Manson concluded that there was a definite correlation between sulfate resistance of Portland cement and the quantity of C_3A as calculated. The extensive research at the University of Minnesota established that normal cured concrete of low permeability had good resistance to sulfates when the calculated C_3A in cement is no more than 5.5%.

In 1921 a Committee on the Deterioration of Concrete in Alkali Soils was established by the Council of the Engineering Institute of Canada [10] and financially supported by the Research Council of Canada, the Canada Cement Company, the Canadian Pacific Railroad and the three Prairie Provinces of Canada [11]. After the inspection of field exposed specimens in 1927 [12], it was stated that:

The results obtained from the field exposure tests are quite in accord with those obtained in other field investigations. The main effort should be centered upon research in the chemical laboratory was the original decision of the Committee, and this has proven sound. Few new data or ideas have been brought by the field, but the chemical research has greatly extended our knowledge of the behaviors of cements when exposed to sulfate solutions.

The chemical investigation was conducted under the direction of Dr. Thorvaldson from the University of Saskatchewan [10]. The reaction of the principal minerals in Portland cement clinkers (C_3S, C_2S and C_3A) with water and sulfate solutions were studied. Strength and length change, extraction and microscopical studies were conducted for dilute suspensions of each mineral after exposure in water and salt solutions for different periods of time. The results of these studies with the pure compounds indicated that improved sulfate resistance can be achieved

either by decreasing the alumina content of kiln feed or adding some ferric oxide to it, either of which should decrease the C_3A content of the clinker.

The Portland Cement Association started a large-scale program in 1921 [13]. Approximately 2,000 10 in. by 24 in. concrete cylinders were made in the laboratory and were transported to the field and stored in sulfate soils and waters at Montrose, Colorado and Medicine Lake, South Dakota after two to three months of curing. Laboratory tests using 4 in. by 8 in. cylinders were also carried out under different storage conditions such as water and salt solutions. In short periods of time, serious deterioration of the concrete was observed which are similar to those of the studies conducted by NBS and the University of Minnesota. Over 400 cements with controlled composition were prepared using laboratory kiln and mills [14]. Glass contents were controlled by different cooling and quenching methods. Clinkers with different ratios of C_3S to C_2S, varying free CaO and free MgO contents, low to high C_3A contents with varying C_4AF contents were designed. The performance of specimens exposed to water and 2% solutions of sodium and magnesium sulfates were evaluated. Principal findings with respect to sulfate attack resistance were as follows:

1) Changes in the ratio of C_3S to C_2S lead to little observable effect on expansion in water or sulfate solutions.

2) Expansions of specimens in 2% sodium and magnesium sulfate solutions increase rapidly with increase in C_3A concentration.

3) The effect of C_4AF on the sulfate resistance is usually masked by a much greater effect of C_3A but becomes apparent once the C_3A is controlled at constant concentration. Increases in C_4AF to high values (20~27%) may result in marked acceleration in the length increase rate of specimens.

4) Crystalline C_3A is less resistant to sulfate attack than glass C_3A. In contrary, crystalline C_4AF is more resistant to sulfate attack than glass C_4AF.

2.1.2 MECHANISMS OF SULFATE ATTACK

While the formation of ettringite in regular Portland cement concrete is well established as the cause of deterioration during sulfate attack, the precise mechanism by which ettringite causes expansion is still an open question. The following theories have been formulated for possible explanations.

FORMATION OF ETTRINGITE

The most widely accepted mechanism of sulfate attack ascribes the expansion to the formation of AFt phase (ettringite) within cement paste through a topochemical reaction [15-23]. The alumina-bearing phase reacts with the sulfate ions to form ettringite which occupies a larger volume than the solid which participates in its formation. A local expansion occurred as the ettringite forms, which pushes the surroundings outward.

DOUBLE DECOMPOSITION BETWEEN THE SULFATE AND CALCIUM HYDROXIDE

One sewer constructed in 1890 was so severely deteriorated after a relatively short time in service that portions of it had to be rebuilt [24]. The remaining portions of the sewer were disintegrated in many locations and occasionally portions of the pipe were gone. These observations led to an investigation of chemical reactions involved in the deterioration under the direction of Burke and Pinckey [25]. Based on the chemical analysis results, a hypothesis explaining the deleterious effect of sulfate was proposed as follows:

The chemical reaction of alkali that is destructive to cement work is double decomposition between the various alkali salts and calcium hydroxide, which is an unavoidable constituent, and probably the binding constituent, of all set cement, whether the cement is classed as Portland, natural or slag. This reaction removes greater or lesser amounts of the calcium hydroxide and deposits in its place, in most cases, a molecular equivalent amount of other compounds, which have good cementing properties but occupy more space than calcium hydroxide. This increase in space occupied disrupts the cement, causing it to bulge, crack and crumble.

Typical double decomposition reactions can be represented as follows:

$$Ca(OH)_2 + MgSO_4 + 2H_2O = CaSO_4 \cdot 2H_2O + Mg(OH)_2$$

$$Ca(OH)_2 + Na_2SO_4 + 2H_2O = CaSO_4 \cdot 2H_2O + NaOH$$

Burke and Pinckey found that there is an increase of volume between the reactant and the reaction products. Based on the assumptions that these reaction products tended to be deposited in the space originally occupied by the calcium hydroxide and that these reactions are solid-liquid type as discussed by Hansen [26], they concluded that the volume change of the decomposition cause the cement to expand.

ADSORBED WATER BY GEL SYSTEM

No volume increase was found after careful calculation of the volume of the reactants and reaction products. It seems impossible for a through-solution double decomposition to form solid reaction products, in a capillary pocket, that occupy a greater volume than the pocket plus the volume of the solid calcium hydroxide taking part in the reaction. Therefore the mechanism involving the water adsorption by the gel system was formulated. A colloidal product is surrounded by a shell of adsorbed water due to its surface energy [1]. Precipitation of colloidal solid in the gel pore resulted from the reaction between calcium hydroxide and sulfate disrupted the equilibrium of the water in the pore with the surface energy. The equilibrium can be restored by additional water entering the pore from the surrounding solution to furnish the newly formed solid particles with their shells of adsorbed water. This entrance of water causes the gel system to expand.

UPTAKE OF WATER AND SWELLING OF COLLOIDAL ETTRINGITE

Experimental work demonstrated that the expansion associated with ettringite formation itself was insignificant compared to the expansion when ettringite was exposed to excessive water [27]. Scanning microscopy test by Mehta indicated that the ettringite formed at the presence of lime is colloidal but not lath-like crystals [28]. The colloidal ettringite is characterized by high specific

surface and peculiar structure with a negative net charge as proposed by Moor and Taylor [29]. It was proposed that this colloidal form of ettringite is probably responsible for attracting a large quantity of surrounding water molecules and the cause of interparticle repulsion which eventually result in an overall expansion of the system.

REDUCTION OF THE STIFFNESS OF C-S-H DUE TO THE ADSORPTION OF SULFATE IONS

Since not all the physical manifestation (expansion, cracking, loss of strength and stiffness, and disintegration) of sulfate attack can be adequately explained by the chemical phenomenon of ettringite formation as a result of reaction between sulfate water and hydration product of Portland cement, another less widely accepted theory was forwarded to explain the deterioration associated with sulfate attack [30]. It is speculated that sulfate adsorption on C-S-H surfaces reduces their adhesive ability. Therefore expansion in a system suffered from a loss of stiffness can easily result in large dilatations of the paste and cracking.

SOLID STATE CONVERSION OF C_4AH_{13} TO MONOSULFATE

During the study of the paste hydration of C_3A-gypsum system with and without $Ca(OH)_2$, Chatterji and Grudemo observed that the pastes containing $Ca(OH)_2$ cracked before three months while those without $Ca(OH)_2$ remained intact. X-ray diffraction and electron-optical examination revealed that the initial sulfate-bearing compound was ettringite but the final one was calcium aluminate monosulfate ($C_3A \cdot CaSO_4 \cdot xH_2O$). The expansion seems to be connected with the formation of monosulfate at the expense of ettringite. Based on these observations, they proposed that the sulfate explanation is resulted from the solid state conversion of C_4AH_{13} to monosulfate [31].

$$C_4AH_{13} + SO_4^{2-} + aq = C_3A \cdot CaSO_4 \cdot H_{12} + 2OH^- - aq$$

There is a net volume increase of about 14% during the solid state conversion. In the case of C_3A-gypsum system, part of the C_4AH_{13} crystal will dissolve and diffuse out to other part of the matrix

and will be precipitated. The increase in volume will be accommodated by this dissolution-diffusion-precipitation process. However, the concentration of lime is high for the case of C_3A-gypsum-$Ca(OH)_2$ mixtures. The solubility of C_4AH_{13} is depressed thus the accommodative process is inoperative. Consequently there will be a disruptive expansion.

OSMOTIC FORCES

After discussing theories of sulfate resistance, Thorvaldson made the following statement [32]:

Many observations such as these suggest that volume changes in mortars are controlled by osmotic forces concerned with the swelling of gels, that the chemical reactions condition the gel system and destroy cementing substances while the formation of crystalline material is incidental to these chemical reactions, and that the increased resistance to volume changes with increased richness of mix may not be primarily due to decreased permeability but rather to the more prolonged maintenance of conditions within the mortar unfavorable to the swelling of the gels.

2.2 DETERIORATION MECHANISMS OF CONCRETE DUE TO SECONDARY MINERAL FORMATION

A significant problem associated with concrete deterioration is the formation of secondary minerals such as ettringite and thaumasite long after the concrete has hardened [33]. The formation of those minerals leads to significant expansion resulting in cracking when the stress in the concrete matrix exceeds its tensile strength. The secondary minerals must be differentiated from the primary minerals normally formed in the first days of cement hydration. For instance, primary etrringite is formed by the reaction between gypsum and the alumina phase of the cement (tricalcium aluminate $3CaO{\cdot}Al_2O_3$ abbreviated as C_3A). It turns into monosulfoaluminate ($3CaO{\cdot}Al_2O_3{\cdot}CaSO_4{\cdot}12H_2O$) which is a more stable form of sulfoaluminate, and finally into hydrogarnet (C_4AH_{13}) [34]. The remaining sulfate ions are trapped in the structure of the C-S-H gel. Secondary ettringite can be expansive and its volume is three to eight times larger than that of the original solid [35]. Though the mechanisms involved remain controversial, the delayed

formation of these minerals is believed by many researchers to cause the expansion and premature deterioration of concrete [36-43].

2.2.1 OXIDATION OF SULFIDE-BEARING AGGREGATE AND PRIMARY EXPANSION

Secondary mineral formation is strongly dependent on the availability of sulfate which can be supplied either from internal or external sources. External sources include natural or polluted ground water, moisture in soils and sulfate-rich acid rain [44-45]. Sulfur dioxide from the combustion of motor fuels and the sulfate impurities of deicing salt are also potential external sources [46]. Internal sources are primarily sulfate or sulfide rich components of concrete, such as cement and aggregate. SO_3 content in cement is usually within the range of 2.5 to 4.0 wt.% which is considered safe to avoid delayed ettringite formation [47]. Therefore aggregates rich in sulfide become critical internal sources of sulfur for delayed mineral formation. Pyrite (FeS_2) and pyrrhotite ($Fe_{1-x}S$) are the most common iron sulfide in nature and are common minerals disseminated in various rock types. Oxidation of these sulfides at the presence of water and oxidant (oxygen or ferric ion) leads to series of chemical reactions and to the formation of products with larger volume than the initial reactant [48].

Table 2-1 summarizes the expansive oxidation reactions of these sulfides which have been referred as "primary expansion" [49]. It is worth noting that volume changes listed in **Table 2-1** represent maximum expansion at complete reaction thus it overestimates the potential volume expansion. From the thermodynamic stability point of view, ferrihydrite ($Fe(OH)_3$) is the predominant sulfide oxidation product under the alkaline conditions that are representative for concrete [50].

Table 2-1 Primary expansion induced by the oxidation of pyrite and pyrrhotite in aqueous systems and their associated volume changes. Pyrrhotite reactions balanced for x=0.125, after [49]

	Reaction	ΔV_{solids} (cm^3/mole of sulfide)
Pyrrhotite	$8F_{1-x}S + \frac{31}{2}O_2 + 8H_2O \rightarrow 7(FeSO_4 \cdot H_2O) + SO_4^{2-} + 2H^+$	209.96
	$8F_{1-x}S + 21O_2 + 11H_2O \rightarrow 7Fe(OH)_3 + 8SO_4^{2-} + H^+$	6.04
	$8F_{1-x}S + \frac{67}{4}O_2 + \frac{25}{2}H_2O \rightarrow 7FeOOH + 8SO_4^{2-} + 16H^+$	0.64
Pyrite	$FS_2 + \frac{9}{2}O_2 + 2H_2O \rightarrow FeSO_4 \cdot H_2O + SO_4^{2-} + 2H^+$	209.96
	$FS_2 + \frac{18}{4}O_2 + 2H_2O \rightarrow Fe(OH)_3 + 2SO_4^{2-} + H^+$	3.05

2.2.2 INTERNAL SULFATE ATTACK AND SECONDARY EXPANSION

It can be seen from **Table 2-1** that sulfate and hydrogen ions are released during oxidation. In hardened concrete, hydrogen ions attack the matrix and react with portlandite ($Ca(OH)_2$), a hydration product of Portland cement, to gypsum ($CaSO_4 \cdot 2H_2O$). Gypsum then reacts with the alumina phase in cement (tricalcium aluminate $3CaO \cdot Al_2O_3$) resulting in the formation of monosulfoaluminate ($C_4\overline{A}\overline{S}H_{12}$) and, eventually, ettringite ($C_6\overline{A}\overline{S}_3H_{32}$). The expansions of these secondary minerals have been referred as "secondary expansion" [50]. **Table 2-2** lists these secondary expansion reactions in increasing order of volume expansion. The predominance of one or another reaction is controlled by pH and the availability of sulfate ions. Formation of gypsum is preferable at pH<10.5. Due to the strong alkalinity of concrete it is unlikely that gypsum is a principle contributor to secondary expansion.

It is worth pointing out that under alkaline conditions in concrete, ferrihydrite is the most stable product of sulfide oxidation. Its volume increase (**Table 2-1**) is small compared to that of

monosulfate or ettringite (**Table 2-2**) resulting from the reaction of sulfate ions with portlandite and tricalcium aluminate, respectively.

Table 2-2 Secondary expansion reactions due to delayed formation of ettringite and their associated volume changes, after [49]

Reaction	ΔV_{solids} (cm^3/mole of sulfide)
$CH + \overline{S} + 2H^+ \rightarrow C\overline{S}H_2$ (gypsum)	41.63
$CH + C_3A + \overline{S} + 11H \rightarrow C_4A\overline{S}H_{12}$ (monosulfoaluminate)	182.89
$3CH + C_3A + 3\overline{S} + 29H \rightarrow C_6A\overline{S}_3H_{32}$ (ettringite)	172.19

2.3 HISTORICAL INVESTIGATION

Scientific knowledge of deteriorating concrete home foundations due to internal sulfate attack and secondary expansion is limited, as evidenced by the scarcity of written work, and there remains no broadly recognized scientific consensus about the problem. Most published literatures of concrete deterioration associated with the expansion of pyritic rocks are linked to external causes, usually cracking and uprising of concrete buildings lying on swelling rock foundation or on a swelling rock fill. In very few cases concrete deterioration is caused by internal conditions, such as the expansion of sulfide rich aggregates as a result of the oxidation of pyrite or pyrrhotite [51-53].

To the best knowledge of the authors, the first internal sulfate attack induced by sulfide containing aggregate was reported in the Oslo region of Norway, 1959 [54].

Numerous cases of concrete deterioration due to sulfide containing rocks have been reported in Canada. The first deterioration cases associated with heaving of rock foundations due to pyrite oxidation were published during the 1970s [55-56]. In the providence of Quebec, deterioration related to pyrite oxidation was first found in the region of Quebec City in 1983 and Matane in

1984 [57]. The cases in the Montreal area were officially reported in the 1990s [58-59]. The first symposium concerning harmful pyritic rock fills was held in May 1997 by the Montreal section of the Association of Engineering Geologists (AEG). More recently, premature deterioration of concrete foundations two to four years after construction in the Trois-Rivières area (Québec, Canada) were reported [60]. Rodrigues et al. investigated the importance of thaumasite formation on the reaction mechanism of concrete damage resulted from the oxidation of sulfide containing aggregates [61].

Although sulfide containing aggregates induced premature deterioration of concrete, only a limited number of scientists were aware of this problem before 1998. However, increasing interests arise as more and more damage is reported worldwide. Lee et al. investigated Iowa (USA) highway concrete deterioration in 2005 [62]. Oliveira et al. reported the downstream face and galleries damage of the Graus Dam (Spain) in 2014 [63].

2.4 STANDARDS OF IRON SULFIDES IN AGGREGATE FOR CONCRETE

In Europe, there are different standards regulating the content of iron sulfides in aggregates for concrete. Spanish Regulations of Structural Concrete (EHE), in force between 1999 and July 2008, prohibits the use of aggregates containing oxidizable sulfur compounds (Article No. 28). It is clarified in the comments section that "*oxidizable sulfurs (e.g. pyrrhotite, marcasite, and some forms of pyrite), even in small quantities are very damaging to concrete since, as through oxidation and hydration, they form sulfuric acid and iron oxide/hydroxide minerals*". Similar requirements are stated in ASTM C294-05 (Section No. 13): *"marcasite and certain forms of pyrite and pyrrhotite are reactive in mortar and concrete, producing a brown stain accompanied by an increase in volume that has been reported as a source of popouts in concrete"*. It is worth noting that no obligatory European standard was in place in 1998. Recent European standard EN 12620:2008 (Section 6.3.2) makes the following statement: *"should the presence of oxidizable iron sulfides in the form of pyrrhotite be detected, the sulfur content provided by them, expressed*

in S, will be lower than 0.1%". This is the same requirement as that in the updated Spanish Regulations of Structural Concrete EHE-08 (Section 28.7.3). Notably, American regulators have not responded to either scientific findings or incidents of sulfur attacks by enacting regulations in building codes or statutes that limit the amount of iron sulfides in concrete.

3. ON SITE SURVEY

A list of candidate residences had been preselected to conduct onsite inspection and collect core samples based on their construction date, degree of deterioration and geographical distribution. The distribution of these homes is illustrated in **Fig. 3.1**. In this report seven homes (marked as 1 through 7 in **Fig. 3.1**) from the preliminary list were chosen for further investigation. Typical deterioration symptoms are summarized as follows:

- map cracking with wide opening and/or significant deformation of the wall
- whitish formation of minerals at the vicinity of cracking surface
- reddish - brown discoloring

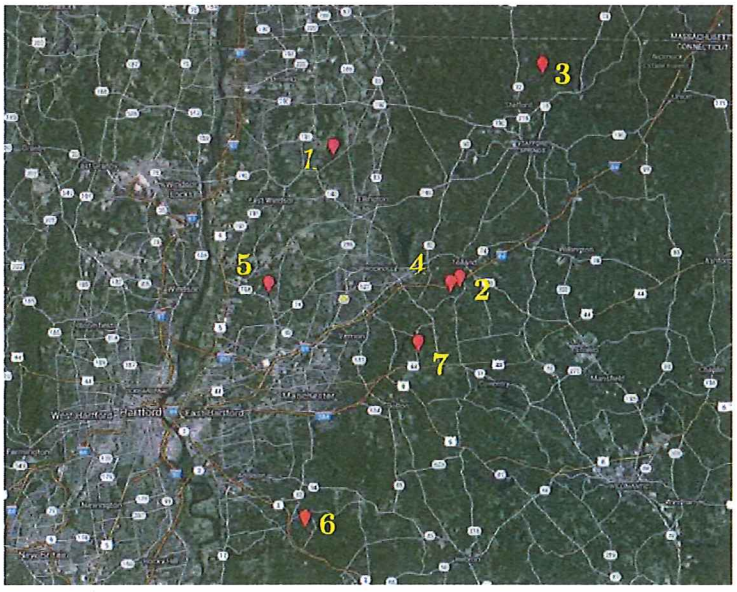

Fig. 3.1 Geographical distribution of candidate housing

a) map cracking

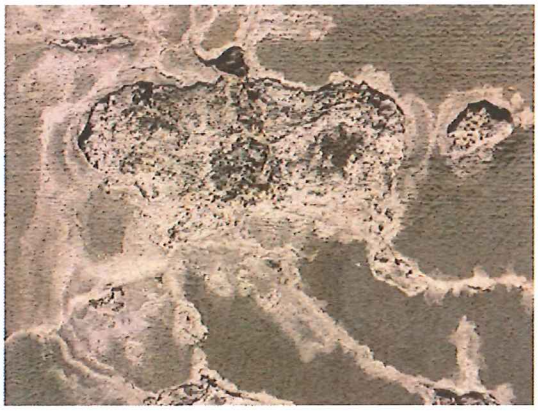

b) Abundant whitish powder

c) reddish – brown discoloring

d) crack opening (>4mm)

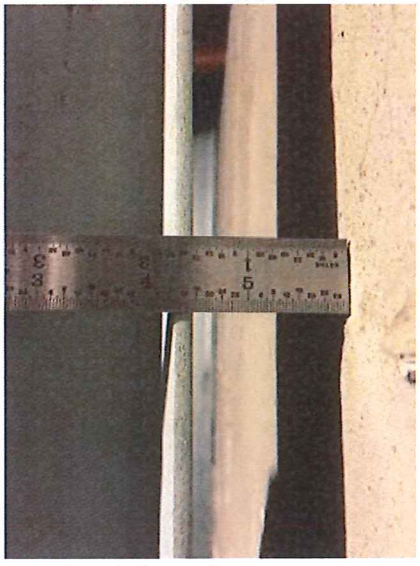

e) significant deformation of the concrete foundation wall

Fig. 3.2 Typical symptoms of deteriorated foundation

Since the inspected houses where core samples were taken show similar symptoms, only visual inspection was conducted for additional 14 houses. Soil samples were also taken and examined in the soil laboratory at the University of Connecticut.

4. COMPRESSIVE STRENGTH

4.1 SAMPLE COLLECTION

Cylinder cores with a diameter of 3 inch and a minimum length of 6 inch were drilled out of the walls both at relatively intact and deteriorated areas for compressive strength test. The lengths of the cores drilled out of slabs were restrained by the actual thickness of the slab and ranged from 3 to 4 inches. An experienced third party contractor was hired to carry out the coring process (**Fig. 4.1**). In general, at least 9 concrete samples were cored from the foundation wall of each house.

Fig. 4.1 Coring process carried out by a third party contractor

4.2 SPECIMEN PREPARATION AND COMPRESSION TESTING

The collected samples were cut to 6 inch in length using a diamond saw. Special emphasis was placed in achieving high quality of the load face ends in terms of planeness and perpendicularity. After cutting the load faces were ground (**Fig. 4.2b**) and capped with sulfur (**Fig. 4.2c**). The capping process was conducted following ASTM C617. The cutting and grinding/polishing equipment are shown in **Fig. 4.3a** and **b** (MetLab Corporation – Metpol 300-1V) respectively.

a) originally collected b) after cutting c) after sulfur capping

Fig. 4.2 Specimen preparation procedure

a) Cutting saw

b) Rotary grinding and polishing machine

c) Load frame

Fig. 4.3 Specimen preparation and test equipment

Once the preparation procedure had been completed the specimens were placed and carefully aligned between the load platens of a hydraulic compression load frame (**Fig. 4.3c**) with a capacity of 400,000 pounds (1780 kN) of force. The machine displacement was set to a rate of 0.5 mm/min. Failure usually occurred within 1-2 minutes. Compressive strength was determined in accordance to ASTM C39.

4.3 TESTING RESULTS

The compressive strength of individual specimens is summarized in **Table 4-1** along with the average (AVG), standard deviation (STD) and coefficient of variation (CV). It can be seen that most of the CV for intact (IT) zone is smaller than 9% as required by ASTM C42. The CV for severely deteriorated (SD) area is significantly higher than 9% while the CV for moderately deteriorated (MD) zone lies in between. It is worth noting that due to the severe deterioration of the concrete foundation wall, some of the collected core samples are just a group of pieces of disintegrated aggregates with attached matrix (**Fig. 4.4**) thus the compressive strength of such samples are 0 MPa and the compressive strength reduction is considered as 100%. As summarized in **Table 4-1**, the compressive strength reduction of concrete foundation wall ranges from 27% to 100%.

Fig. 4.4 Completely disintegrated core sample of concrete foundation wall– house 1

Table 4-1 Summary of compressive strength test result

House	Wall/Slab	Location	Individual (MPa)	AVG (MPa)	STD (MPa)	CV (%)
1	Wall	SD	0	-	-	-
		SD	0	-	-	-
		SD	0	-	-	-
		IT	21.8	21.0	1.4	6.7
		IT	21.9			
		IT	19.4			
		IT	18.7	18.9	0.3	1.7
		IT	18.8			
		IT	19.3			
	Slab*	IT	50.8	49.1	3.4	6.9
		IT	51.3			
		IT	45.2			
2	Wall	SD	15.7	14.3	1.6	10.9
		SD	12.6			
		SD	14.6			
		IT	16.7	19.5	3.8	19.7**
		IT	18.5			
		IT	17.7			
		IT	25.2			
	Slab*	IT-R	34.0	36.7	2.3	6.2
		IT-R	31.6			
		IT-R	30.2			
3	Wall	SD	11.1	-	-	-
		SD	9.6	11.3	1.9	16.7
		SD	13.4			
		MD	17.8	15.2	2.3	14.9
		MD	13.4			
		MD	14.5			
		IT	27.6	26.0	1.5	5.9
		IT	24.5			

		IT	25.8			
		IT	43.3			
	Slab	IT	38.6	38.9	4.2	10.9
		IT	34.9			
		SD	-	-	-	-
		SD	-	-	-	-
		SD	-	-	-	-
		MD	17.2			
	Wall	MD	18.5	17.4	0.9	5.4
		MD	16.6			
4		IT	27.0			
		IT	22.6	24.5	0.1	9.3
		IT	23.8			
		IT	32.1			
	Slab	IT	36.1	34.8	0.1	6.7
		IT	36.2			
		SD	0	-	-	-
		SD	0	-	-	-
		SD	0	-	-	-
		MD	-	-	-	-
	Wall	MD	15.0	13.3	2.5	18.7
		MD	11.5			
5		IT	22.6			
		IT	19.4	21.0	1.6	7.7
		IT	20.8			
		IT	38.4			
	Slab	IT	37.4	37.1	1.4	3.7
		IT	35.6			
		SD	11.1			
		SD	13.7	12.3	1.3	10.3
6	Wall	SD	12.2			
		MD	10.9			
		MD	14.1	14.1	3.2	22.5

		MD	17.3			
		IT	13.6			
		IT	12.3	13.6	1.3	9.7
		IT	14.9			
		IT	38.1			
		IT	28.4	31.1	6.1	19.6
	Slab	IT	26.8			
		C	38.1			
		C	28.4	25.7	5.2	20.3
		C	26.8			
		SD	8.8			
		SD	13.5	10.3	2.8	27.7
		SD	8.4			
		MD	24.9			
	Wall	MD	24.2	22.0	4.5	20.4
		MD	16.8			
7		IT	-	-	-	-
		IT	-	-	-	-
		IT	-	-	-	-
		IT	27.5			
	Slab	IT	27.2	26.0	2.2	8.6
		IT	23.5			

*A strength correction factor was applied due to the smaller than 1 length to diameter ratio (*l/d*) in accordance with ASTM C42/C42 M.

** This higher than standard allowed (9%) coefficient of variation (CV) may be attributable to the inhomogenity of concrete or disturbance of the bond between the mortar and coarse aggregate during the coring process.

5. ASSESSMENT OF THE QUARRY AGGREGATE

5.1 XRD EXAMINATION

5.1.1 SAMPLE PREPARATION AND TEST SET UP

Aggregate with a brown color, indicating signs of oxidation, were selected for this investigation (**Fig. 5.1a**). Brown parts were separated from the original coarse quarry aggregate (**Fig. 5.1b**), ground in a mortar (**Fig. 5.1c**) and sieved (**Fig. 5.1d**) through a series of sieves. Powder smaller than 45 μm were collected [34]. Prior to the XRD analysis, samples were set down and compacted on the rough surface of a plastic block to be randomly disoriented (**Fig. 5.1e**). Prepared sample was mounted (**Fig. 5.1f**) and tested in a Bruker D2 Phaser X-ray diffractometer as shown in **Fig. 5.2**. Cu Kα radiation (λ=1.5418Å) generated at 10 mA and 30 kV is used in this research. The mineralogical phase of aggregate is analyzed by a commercial package Jade®.

a) piece of coarse quarry aggregate with a brown color

b) parts separated from the original crushed concrete piece

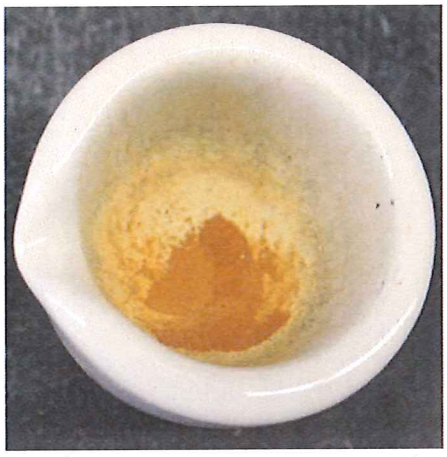

c) ground sample using mortar and pestle

d) sieved sample

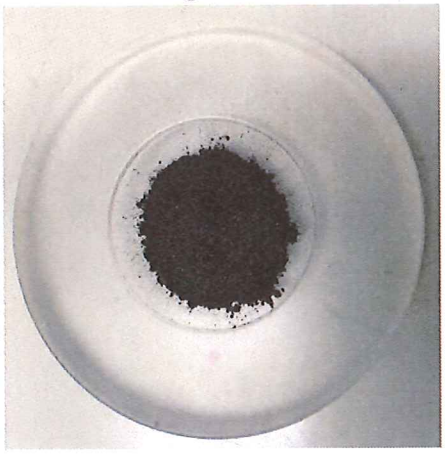

e) sample in the vehicle for XRD test

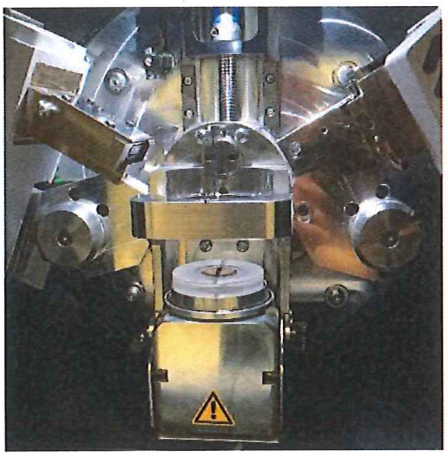

f) sample mounted for XRD test

Fig. 5.1 Sample preparation for XRD testing

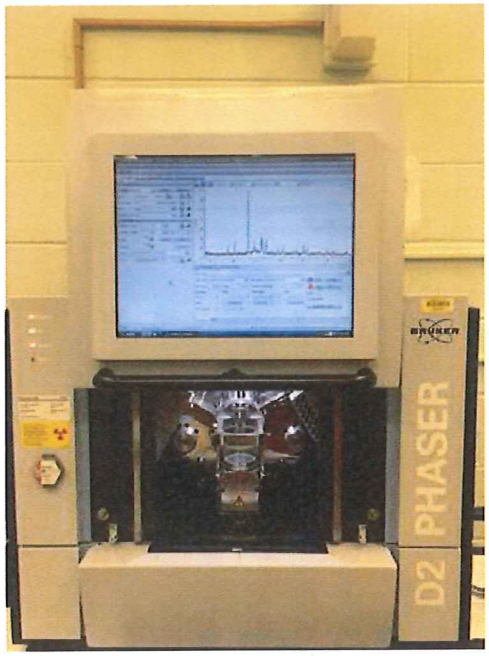

Fig. 5.2 Bruker D2 phaser X-ray diffractometer

All specimens were step-scanned as random powder mounts from 11° to 80° at 0.02° 2θ steps integrated at 1s $step^{-1}$. This step size and scanning time was selected based on the consideration of both detailed spectrum and appropriate testing time. Three scanning times (0.1s, 1s and 10s) were initially selected. For the purpose of comparison, the XRD patterns are normalized with respect to their peak intensity. **Fig. 5.3** compares the normalized XRD patterns at different scanning time. It can be seen that the 0.1s scanning time is too short and the background noise level is high. Increased scanning time (1s and 10s) leads to lower noise level and smoother XRD pattern. Increase of scanning time from 1s to 10s does not result in profound further improvement of the XRD pattern. The effect of scanning time on the XRD pattern can be seen more apparently once the relative difference is compared (**Fig. 5.4**). The relative difference is defined as the ratio of the difference between the XRD pattern of interest and the XRD pattern with 10s scanning time to the normalized XRD pattern with 10s scanning time. It is observed that the relative difference for the XRD pattern with 0.1s scanning time is at the level of 30% and can be as high as 75%. In contrast, the relative difference for the XRD pattern with 1s scanning time is at a low level of

10%. Therefore 1s scanning time is selected for all the XRD testing in this research. It is worth noting that it is based on the assumption that the XRD pattern with 10s scanning time represents the real XRD pattern.

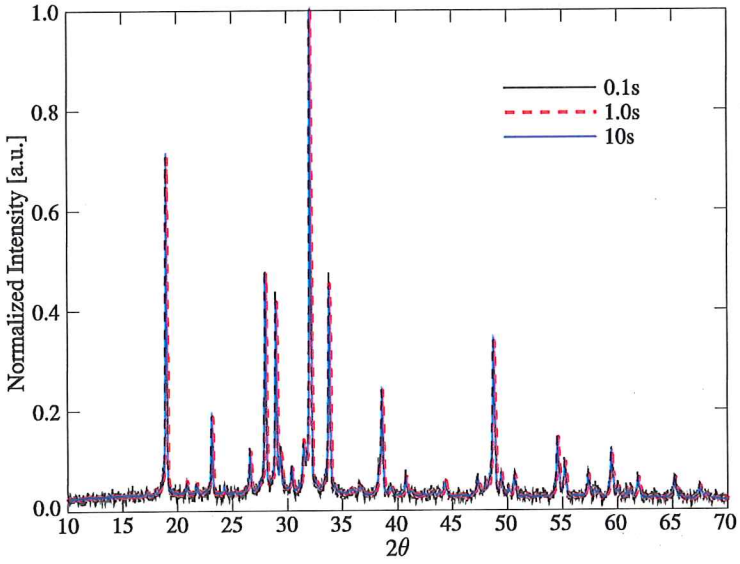

Fig. 5.3 Normalized XRD pattern at different scanning time

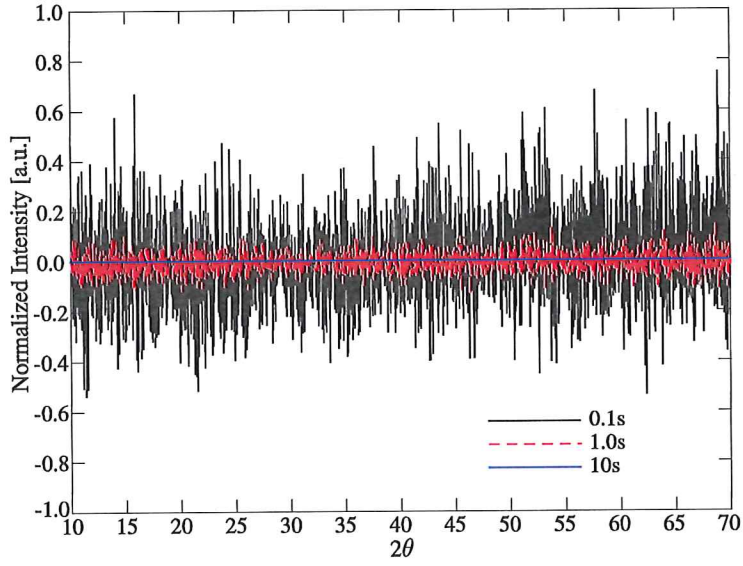

Fig. 5.4 Relative difference plot for different scanning time

5.1.2 TEST RESULTS

Typical XRD pattern for the coarse quarry aggregate is illustrated in **Fig. 5.5**. It can be seen that no pyrrhotite was detected. This is attributable to the limitation of the XRD test that phases with a

concentration below 5% is not detectable. Therefore supplementary XRF and SEM-EDX tests were carried out.

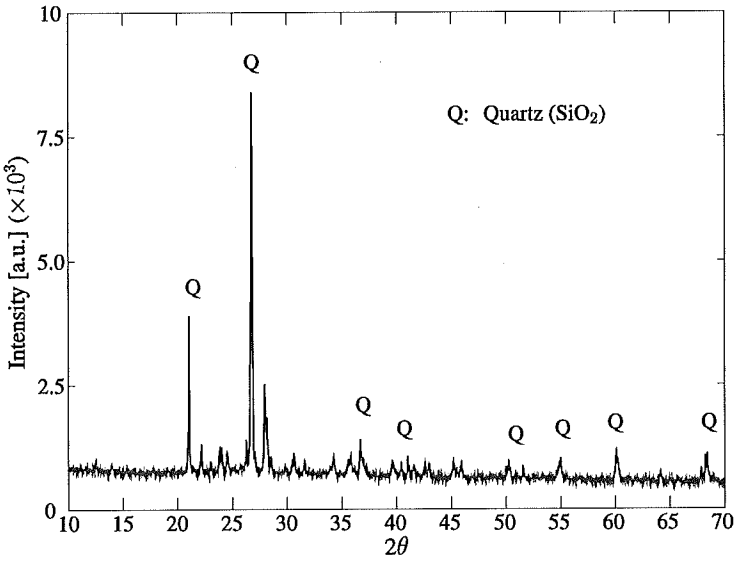

Fig. 5.5 Typical XRD pattern of the coarse quarry aggregate

5.2 XRF

To overcome the limit of XRD test, elemental analysis using XRF technology was conducted for both the quarry aggregate showing signs of pyrrhotite and the reference aggregate. Emphasis was laid on iron and sulfur elements which iron sulfides consists of. The following sections present detailed information on the sample preparation and test results.

5.2.1 SAMPLE PREPARATION AND TEST SET UP

The coarse aggregate was processed for XRF test following the procedures described in section 5.1.1. The prepared powder was put in a plastic cell with a diameter of 31mm and covered with a special thin film 6μ in thickness designed for XRF test (**Fig. 5.6**). The covered cell was then mounted on a INNOV-X Systems analyzer for XRF test.

(a) Sample in cell covered by thin film

(b) INNOV-X Systems XRF analyzer

Fig. 5.6 Sample preparation and test set up for XRF test

5.2.2 TEST RESULTS

The XRF test results are listed in **Table 5-1**. It can be seen that a significant amount of sulfur (2.542% on average) was detected in the quarry aggregate with brown color while no sulfur was detected for the reference aggregate. Iron was detected in both types of aggregate. However, the amount in the brown aggregate is several orders of magnitude higher than that in the reference aggregate. The higher level of sulfur and iron in the brown aggregate than the reference aggregate suggests the existence of iron sulfide in the quarry aggregate.

Table 5-1 XRF test result for the brown and reference quarry aggregate

	Quarry aggregate samples with brown color				Reference quarry aggregate samples			
	1	2	3	Average	1	2	3	Average
S	2.784	2.513	2.326	2.542	-	-	-	-
Fe	6.793	6.415	5.830	6.346	0.00092	0.00091	0.00093	0.00092

5.3 ION CHROMATOGRAPHY

The inclusion of pyrrhotite in and the release of sulfate from quarry aggregate was confirmed by an accelerated oxidation test designed for this investigation. Due to the extremely slow natural oxidation process, quarry aggregate samples were submerged in 40% hydrogen peroxide solution to accelerate the oxidation process. The hydrogen peroxide solution was swapped out and tested

for sulfate concentration using a DIONEX ICS-1100 ion chromatography (**Fig.** 5.7). The use of hydrogen peroxide matrix instead of deionized water delays the retention time and blurs the signal for sulfate (**Fig.** 5.8). To overcome these disadvantages, all samples were diluted ten times using deionized water. The signal for sulfate becomes apparent once the samples were diluted. It is worth noting that the signal for the diluted sample was adjusted by a ratio of the peak signal between original and diluted samples for comparison purpose.

Fig. 5.7 DIONEX ICS-1100 ion chromatography

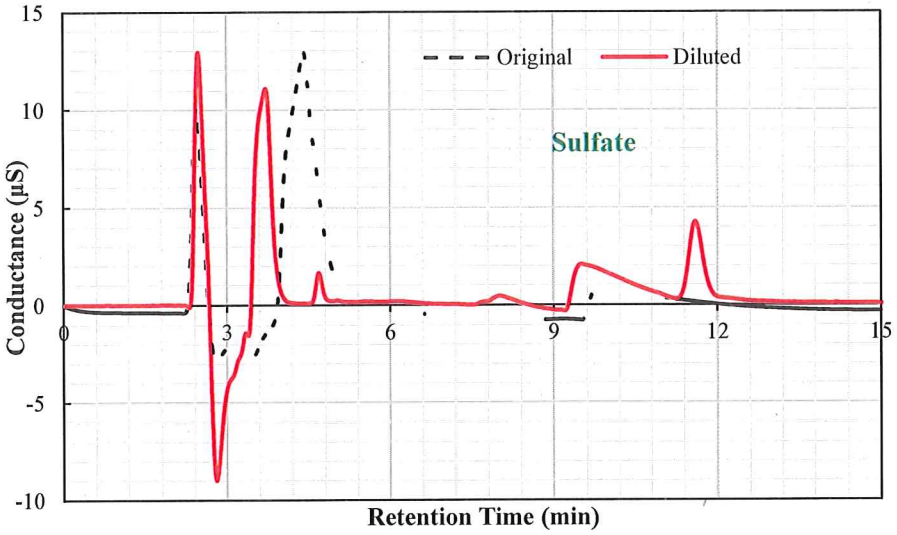

Fig. 5.8 Comparison of IC signal

Increment of the released sulfate due to aggregate oxidation was measured twice a week at predetermined intervals and ceased once the increment is smaller than 5% compared to previous measurement. They were summed up to obtain the accumulated amount of released sulfate. It is worth pointing out that the concentration was normalized by the sample aggregate weight to eliminate the influence of the size of aggregate. The development of concentration of the released sulfate is illustrated in **Fig.** 5.9. It can be seen that the sulfate released by the control sample remains negligible up to the end of the test. In comparison, the normalized sulfate released by the pyrrhotite bearing aggregate increased significantly during the test period. The amount of higher than control aggregate released sulfate through the accelerated aggregate oxidation is a direct evidence of the existence of pyrrhotite in the quarry aggregate.

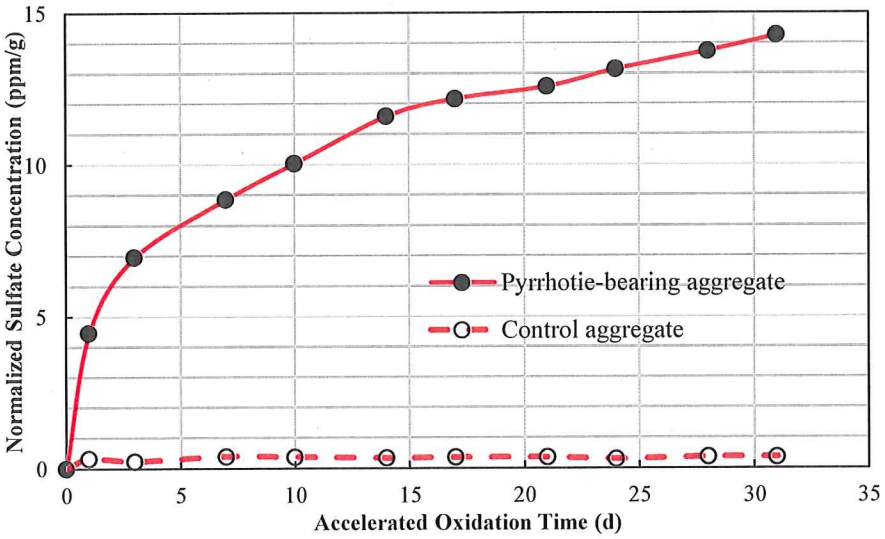

Fig. 5.9 Time history of the normalized concentration of released sulfate

5.4 SEM-EDX

SEM coupled with energy dispersive X-ray test was also conducted to validate the existence of pyrrhotite in the quarry aggregate. SEM-EDX test results confirmed the finding of XRF test results.

5.4.1 SAMPLE PREPARATION

Sub-samples were separated from the coarse quarry aggregate and then dried and impregnated with low viscosity resin (**Fig. 5.10a**) which facilitates the grinding and polishing process. The resin impregnated sample was then ground and polished. To avoid damage to concrete during grinding and polishing, water was used as lubricant and excessive heating was avoided. The polished resin impregnated sample was dried at environmental temperature for 24 hours. To increase the conductivity, the surface of samples was sputter coated with a thin layer of gold/palladium (Au/Pd) alloy (**Fig. 5.10b** and **c**) prior to SEM micro structural examination and EDX elementary analysis. **Fig. 5.11** shows the Teno Field Emission SEM used in this research. Operating conditions were set at 10~15 kV under secondary electron mode.

a) samples impregnated with low viscosity resin

b) Coating equipment

c) Gold Palladium alloy coating

Fig. 5.10 SEM sample preparation

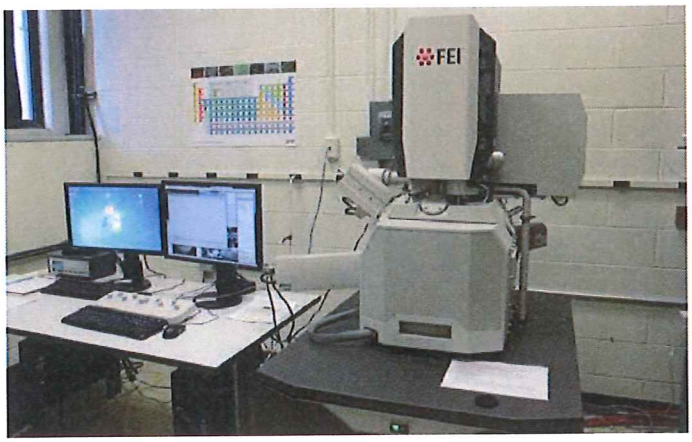

Fig. 5.11 Teno field emission SEM

5.4.2 TEST RESULTS

The SEM image (**Fig. 5.12**) shows two different phases: the dark grey and the light grey phase. Therefore point and area mapping EDX analysis were used to access their elementary composition.

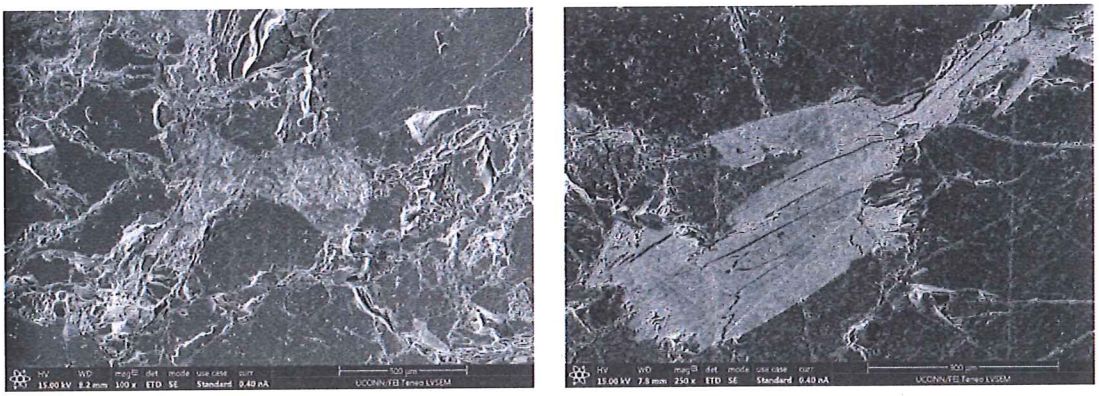

Fig. 5.12 SEM images of the brown aggregate samples

The interface zone between the light grey and dark grey phase, as shown in **Fig. 5.13**, is selected for further analysis. **Fig. 5.14** illustrates the EDX mapping analysis result within the targeted zone (**Fig. 5.13b**) for sulfur (S) and iron (Fe). It can be seen that the light grey phase is rich in sulfur and iron which are the elements for pyrrhotite. In contrast, the dark phase does not demonstrate the existence of any of these elements. Therefore it is hypothesized that this light grey phase is the combination of pyrrhotite. In fact, later XRD analysis of the aggregate from crushed concrete validates this hypothesis. More detailed information can be found in the next chapter.

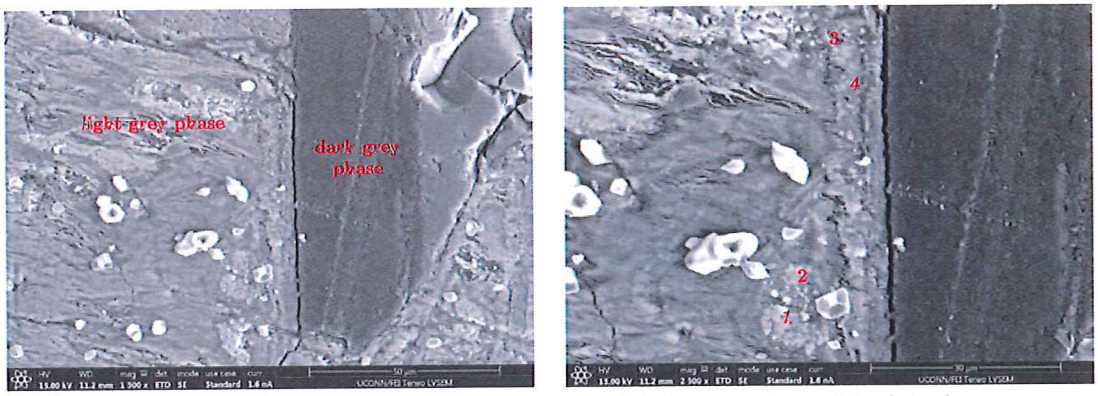

(a) Interface zone between two phases (b) close up view of the interface zone

Fig. 5.13 Interface zone between two different phases

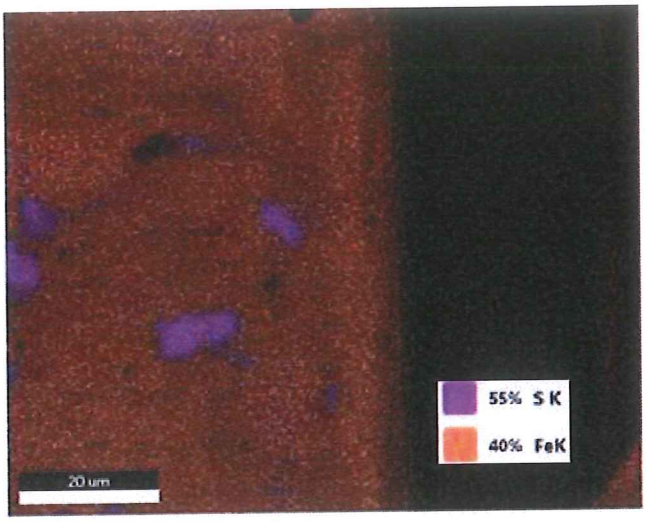

Fig. 5.14 EDX mapping elementary analysis for the interface zone - Sample 1

Four random points (**Fig. 5.14**) in the light grey phase were selected for the EDX point analysis. The results are illustrated in **Fig. 5.15**. Two of the four points demonstrate solely sulfur and iron. It is attributable to the iron sulfides inclusions in the coarse quarry aggregate. The other two points indicates the existence of oxygen along with sulfur and iron. The oxidization of iron sulfide may be the source of oxygen. Similar results were obtained for the other samples. Detailed information can be found in **APPENDIX B**.

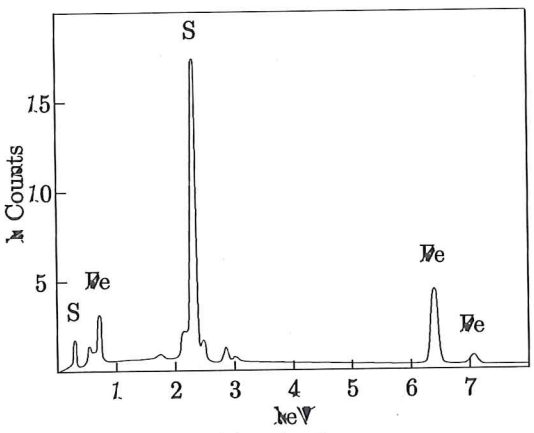

(a) point 1

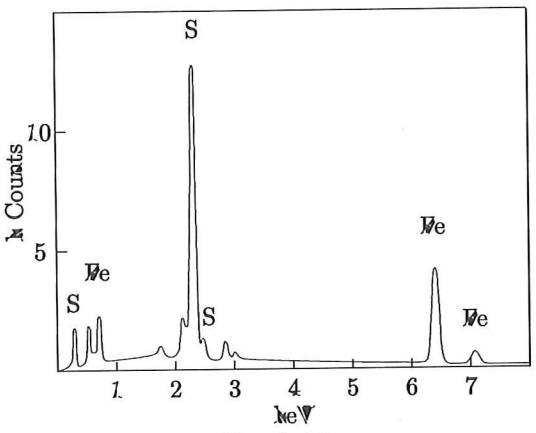

(b) point 2

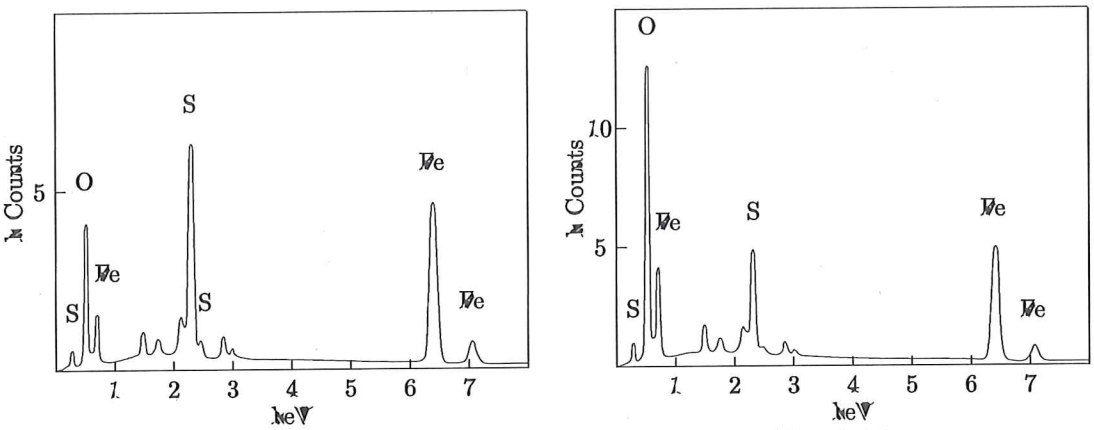

(c) point 3 (d) point 4

Fig. 5.15 EDX spectrum for point 1 to 4

6. MINERALOGICAL ASSESSMENT: AGGREGATES FROM CRUSHED CONCRETE AND FORMATION AT THE VICINITY OF CRACKING SURFACE

6.1 SAMPLE PREPARATION

Brown aggregate, which is a sign of iron sulfide oxidation, were selected for this investigation. Aggregates were separated from cement matrix (**Fig. 6.1a**). Similar procedures described in section **5.1.1** were followed. The whitish formation was scratched off the surface of the deteriorated concrete foundation for XRD testing (**Fig. 6.1b**). All specimens were step-scanned as random powder from 11° to 80° at 0.02° 2θ steps integrated at 1s step^{-1}.

a) separated aggregate b) scratched whitish powder

Fig. 6.1 Sample preparation for XRD testing

6.2 AGGREGATE FROM CRUSHED CONCRETE

Fig. 6.2 through **Fig. 6.5** illustrates the typical XRD pattern of crushed aggregates collected from different houses. As it can be seen from these patterns, most of the aggregates contain pyrrhotite (**Fig. 6.2-Fig. 6.4**). A variety of minerals such as quartz and calcite (**Fig. 6.2**) are also detected. These minerals are common for concrete aggregate. Another important common characteristic is the presence of different pyrrhotite oxidization products, such as ferrihydrite (**Fig. 6.3**), sulfur (**Fig. 6.4**) and goethite (**Fig. 6.5**). It is worth noting that the predominant sulfide oxidation product ferrihydrite [50] under alkaline condition which is typical for concrete is detected (**Fig. 6.3**). This is a strong evidence of pyrrhotite oxidation. The presence of pyrrhotite is potentially oxidized at the presence of water and oxidant (oxygen or ferric ion) forming primary expansion products. More importantly the corresponding release of sulfate can lead to delayed formation of secondary expansive minerals such as ettringite and thaumisite. Both of the primary and secondary expansion products contribute to and ultimately result in the early deterioration of concrete foundation walls. The XRD patterns for the crushed aggregate from different houses are similar and are summarized in **APPENDIX C**.

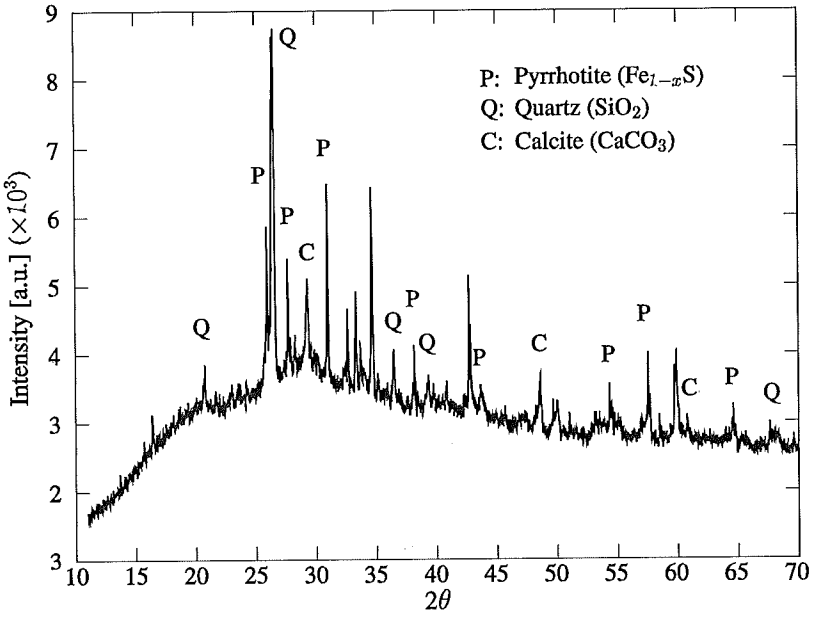

Fig. 6.2 XRD pattern of aggregate indicating the existence of pyrrhotite

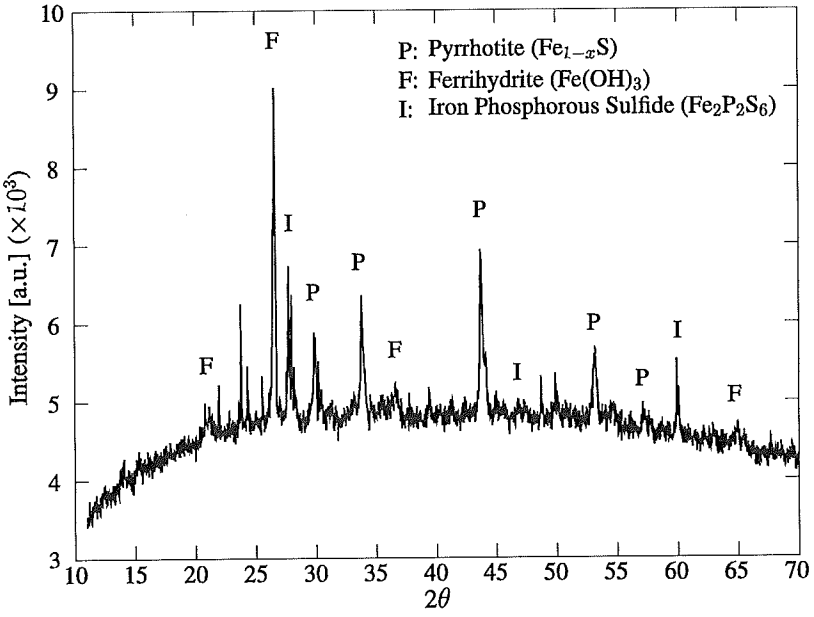

Fig. 6.3 XRD pattern of aggregate showing the oxidization product of ferrihydrite

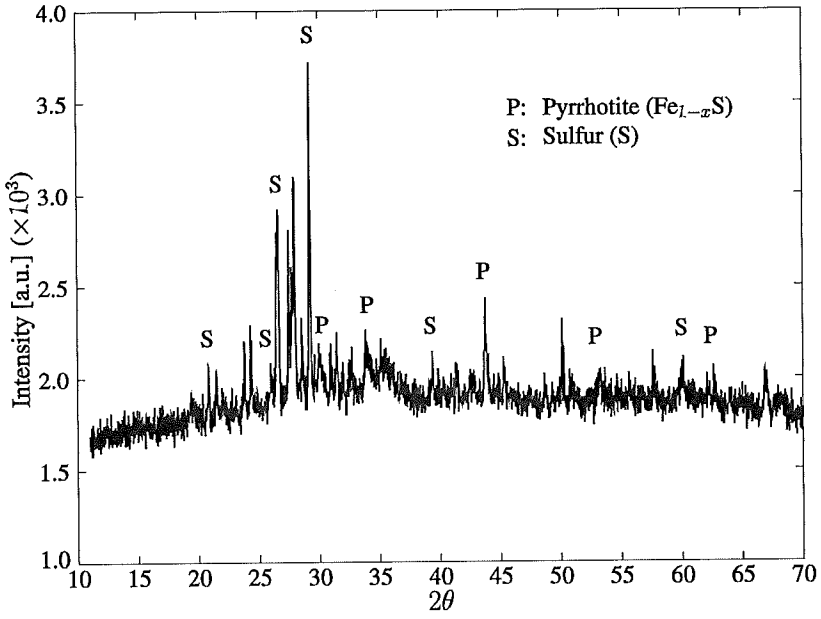

Fig. 6.4 XRD pattern of aggregate showing the oxidization product of sulfur

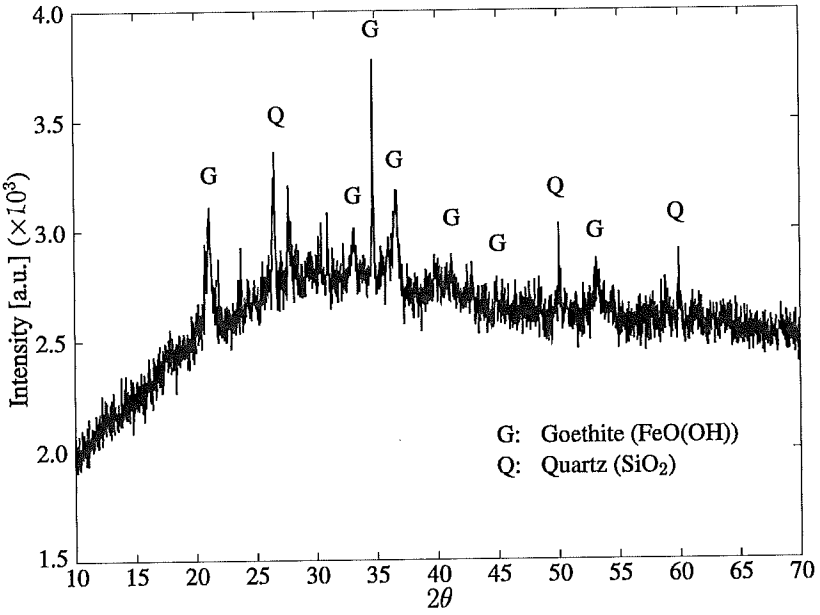

Fig. 6.5 XRD pattern of aggregate showing the oxidization product of goethite

6.3 WHITISH FORMATION AT THE VICINITY OF CRACKING SURFACE

Typical XRD patterns of the whitish formation at the vicinity of cracking surface are present in **Fig. 6.6** and **Fig. 6.7**. It can be seen that quartz (Q) and calcite (C) are detected. This is attributable to remains of aggregate particles mixed with the whitish formation during sample preparation (**Fig. 6.1b**). In addition, gypsum is also observed. This is attributable to the remains of cement matrix during the scratching process of sample preparation. Therefore sulfate rich thenardite (T) and aphthitalite (L) are considered as the primary mineral phases in this whitish powder. The source of sulfate in thenardite and aphthitalite is potentially the released sulfate during the oxidization process of pyrrhotite. It is worth noting that three samples from each inspected houses were tested if enough whitish formation was obtained. Most of the samples demonstrated the existence of sulfate rich minerals such as thenardite (T) or aphthitalite (L) or both. This finding suggests the oxidization of pyrrhotite-bearing aggregate and the potentially delayed formation of minerals such as etttringite and thaumasite.

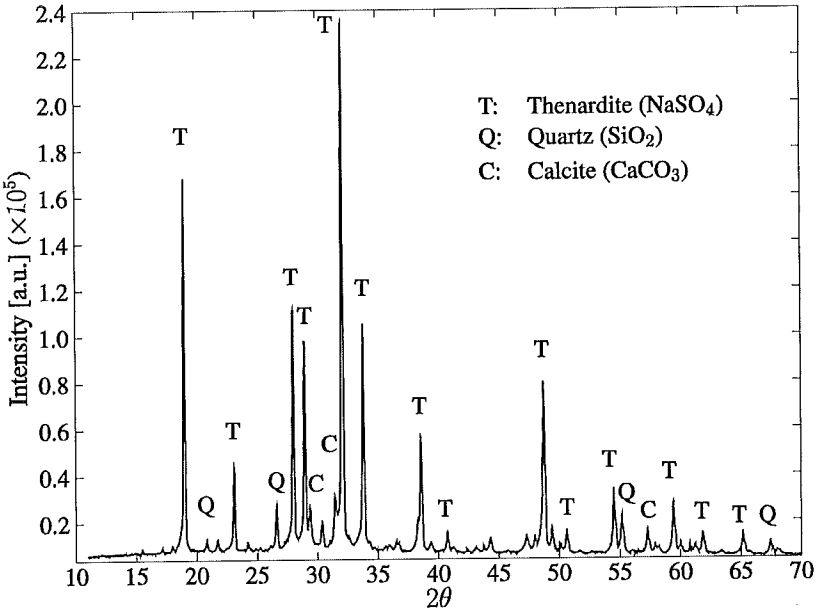

Fig. 6.6 Typical XRD pattern of whitish formation - housing 1

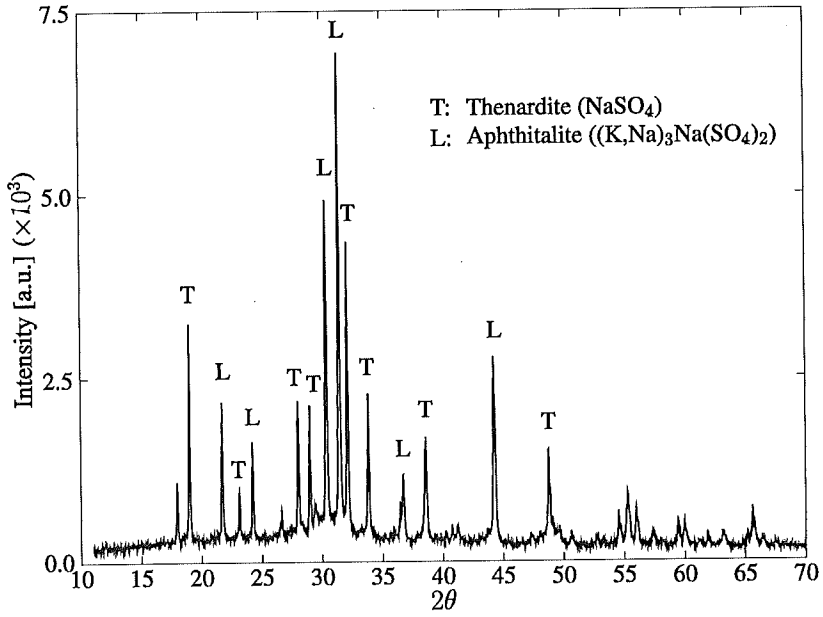

Fig. 6.7 Typical XRD pattern of whitish formation – housing 7

7. MICROSTRUCTURAL INVESTIGATION OF DETERIORATED CONCRETE

Scanning electron microscope (SEM) coupled with energy dispersive X-ray spectrometer (EDXS) is used for the micro structural examination and elementary analysis of deteriorated concrete.

7.1 SAMPLE PREPARATION

Sub-samples were cut out of collected samples and then dried and impregnated with low viscosity resin which serves to restrain against shrinkage cracking and enhances contrast among pores and hydration product. The sample preparation procedures described in section **5.4.1** were followed.

7.2 MATRIX EXAMINATION

Fig. 7.1 presents the micro structure of deteriorated concrete sample at a relatively low magnification of 150. In general, it can be seen that the matrix is very porous. The condition in the interfacial transition zone (ITZ) is the worst with higher than average porosity (the highlighted areas in **Fig. 7.1**). It is hypothesized that a higher amount of oxidation products might be found in the ITZ. Therefore investigating the ITZ might contribute formulating an understanding of the deterioration mechanism of concrete foundation.

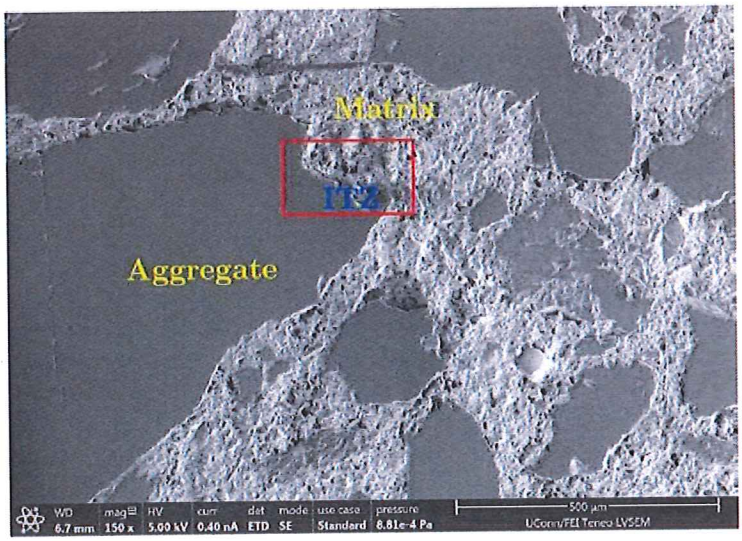

Fig. 7.1 Porous micro structure of matrix

7.3 PYRRHOTITE-BEARING AGGREGATE OXIDIZATION

Sulfate is required for the delayed formation of expansive and thus detrimental secondary minerals. A potential source is the release of sulfate upon oxidation of pyrrhotite contained in aggregate. Previous examination on aggregate has proven the existence of pyrrhotite. In this section, a micro structural assessment of the aggregate was conducted to confirm the oxidization of aggregate. **Fig. 7.2** shows the microstructure of an interfacial transition zone (ITZ) between aggregate and cement paste. Point, linear and mapping EDXS elementary analysis were conducted.

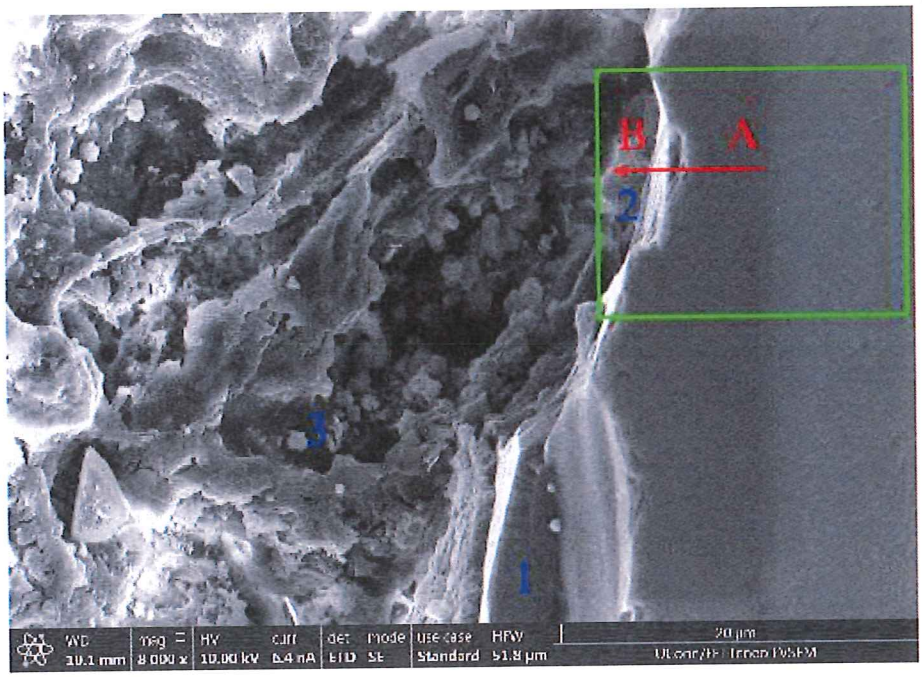

Fig. 7.2 Micro structure of the investigated ITZ

Three random points in the zone of aggregate (point 1), ITZ (point 2) and cement matrix (point 3) were selected and the EDS spectrums of point analysis are illustrated in **Fig. 7.3** through **Fig. 7.5**. It can be seen that at point 1 (**Fig. 7.3**), elemental composition of quartz (SiO_2) is detected with silicon (Si) and oxygen (O). This confirms that the primary mineral of aggregate is quartz. Iron is observed at point 2 (**Fig. 7.4**). This confirms the XRD analysis of aggregate and implies potential pyrrhotite oxidization. Therefore further analysis, such as linear and mapping EDXS, is

performed. It is worth pointing out that no signs of ettringite was found in the cement matrix as demonstrated by the EDS spectrum of point 3 in **Fig. 7.5**.

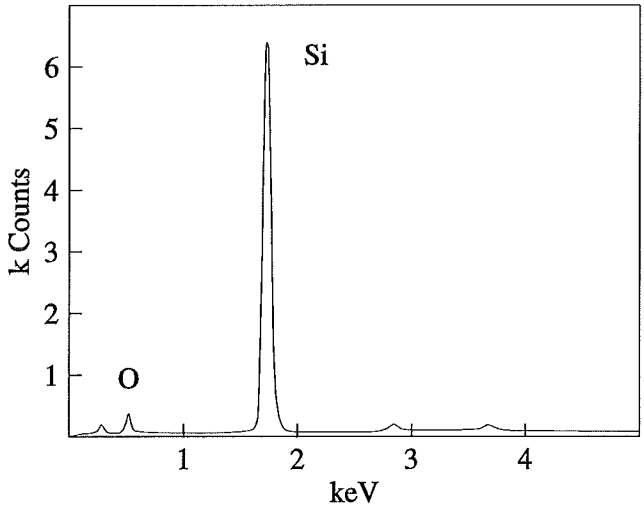

Fig. 7.3 EDX spectrum – point 1

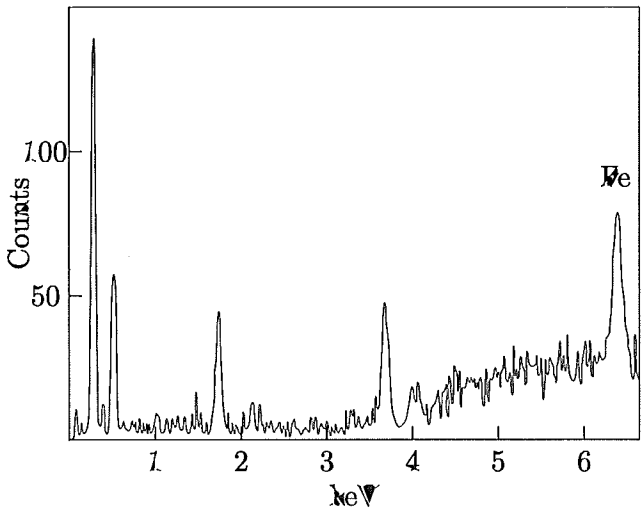

Fig. 7.4 EDS spectrum – point 2

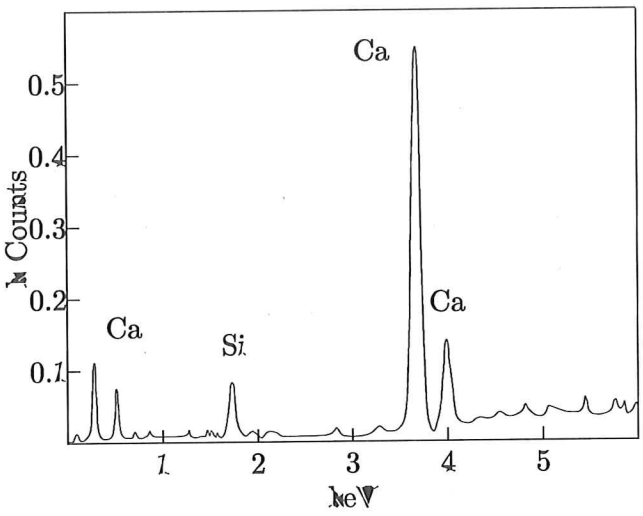

Fig. 7.5 EDS spectrum – point 3

A line at the vicinity of point 2 was picked up for the linear EDXS elementary analysis and the EDS spectrum is shown in **Fig. 7.6**. A decreasing trend of both iron and sulfur elements are detected. The reduction of sulfur is attributable to the release of sulfate after oxidization while the decrease of iron may be explained by the precipitation of ferrihydrite ($Fe(OH)_3$) which is a predominant sulfide oxidation product under the alkaline conditions in concrete [50]. Therefore oxidation of pyrrhotite is validated.

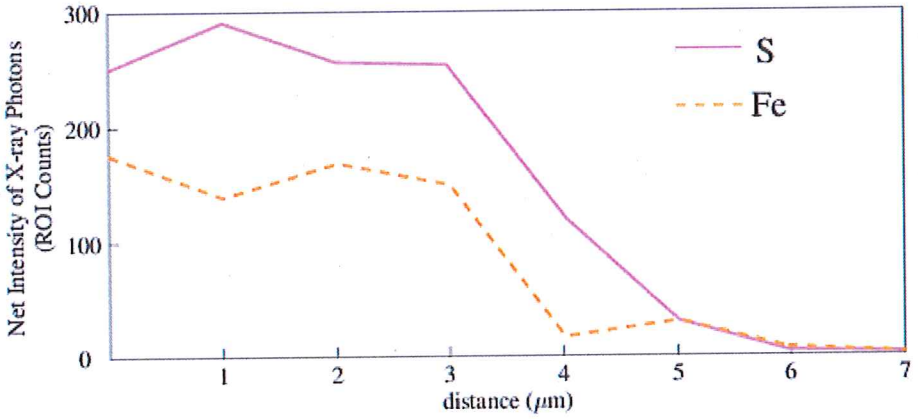

Fig. 7.6 EDS lineal analysis – Line AB from A to B in Fig. 7.2

A zone encompassing point 2 and line AB was chosen for the mapping EDXS elementary analysis to further confirm the occurrence of pyrrhotite oxidation. The result is shown in **Fig. 7.7**. It is observed that iron and sulfur elements are rich at the ITZ between aggregate and cement.

This again confirms the existence of pyrrhotite. Furthermore, the decreasing intensity of iron and sulfur element confirms the oxidation of pyrrhotite.

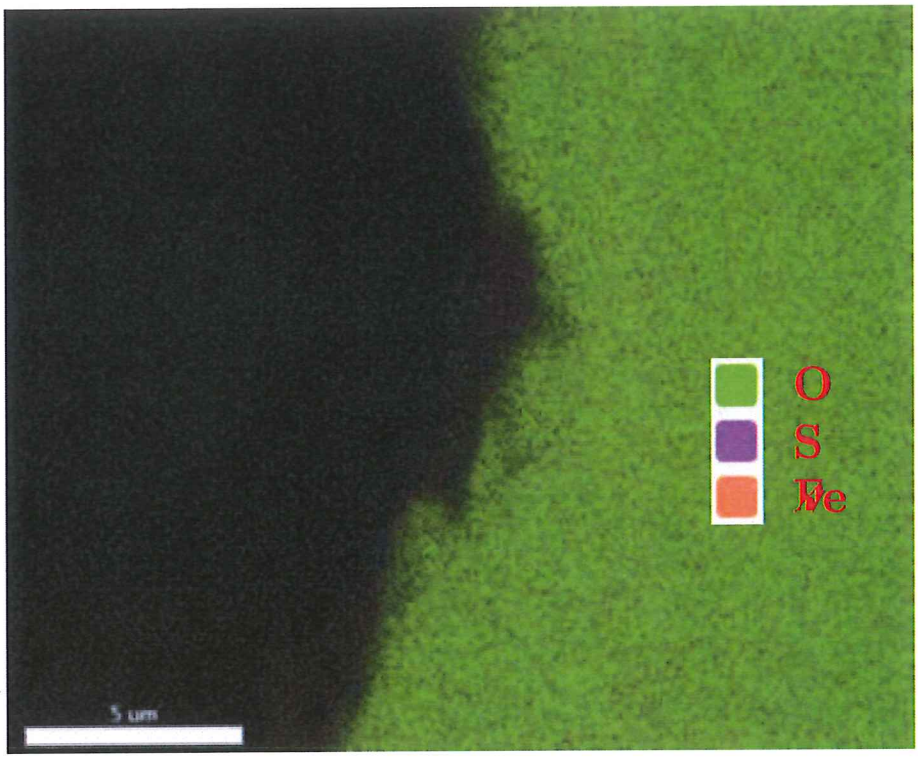

Fig. 7.7 EDS mapping analysis – Rectangular area in Fig. 7.2

7.4 DELAYED FORMATION OF SECONDARY MINERALS

7.4.1 INTERFACIAL TRANSITION ZONE (ITZ)

The microstructure within the ITZ is examined at a high magnification by SEM as shown in **Fig. 7.8**. Large deposits of needle like crystalline material were observed in the ITZ (**Fig. 7.8b**). A point on the aggregate away from the ITZ and one point at the edge of the aggregate are selected as two representative points for EDX elementary analysis of aggregate. Two random points were also selected for the EDX elementary analysis of matrix. Three random points in the ITZ are selected to assess the minerals within the ITZ. The EDX spectrum for aggregate is displayed in **Fig. 7.9**. Elemental composition of quartz (SiO_2) is detected with silicon (Si) and oxygen (O). This confirms that the primary mineral of aggregate is quartz. Composition of iron

and sulfur are detected at the edge of aggregate (**Fig. 7.9b)** confirms the existence of pyrrhotite as validated by the XRD test in section **7.3**.

Fig. 7.11 present the XRD spectrum of the selected points within the ITZ. The EDS spectrums indicate the elemental composition of ettringite, with calcium (Ca), sulfur (S), aluminum (Al) and oxygen (O). It is deleterious to concrete when it is formed after the hardening of concrete due to its expansive nature during formation. Another detrimental mineral found is thaumasite as illustrated in **Fig. 7.12**. Elemental composition of calcium (Ca), silicon (Si), carbon (C), sulfur (S) and oxygen (O) are detected. The carbon may have been supplied by one or a combination of the following (i) calcite present in veins and disseminated through the aggregate (**Fig. 6.2**), (ii) CO_2 trapped in the carbonated surface of the concrete. It must be pointed out that the used EDX spectrometer does not enable analysis of hydrogen (H). The presence of these minerals (ettringite and thaumasite) in the ITZ indicates the delayed formation of these minerals. These secondary minerals may lead to the deterioration of concrete due to the expansive nature upon reaction.

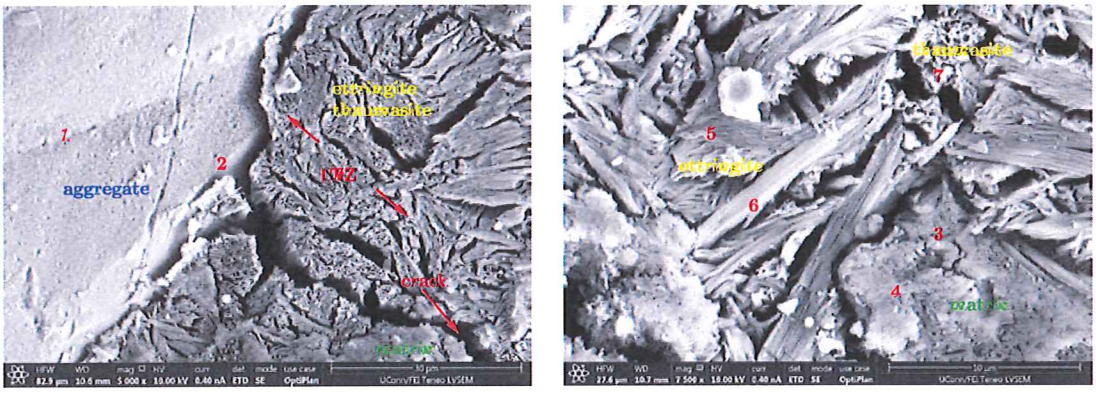

(a) micro structure of the ITZ (b) close up view of the secondary minerals

Fig. 7.8 Secondary minerals in the ITZ

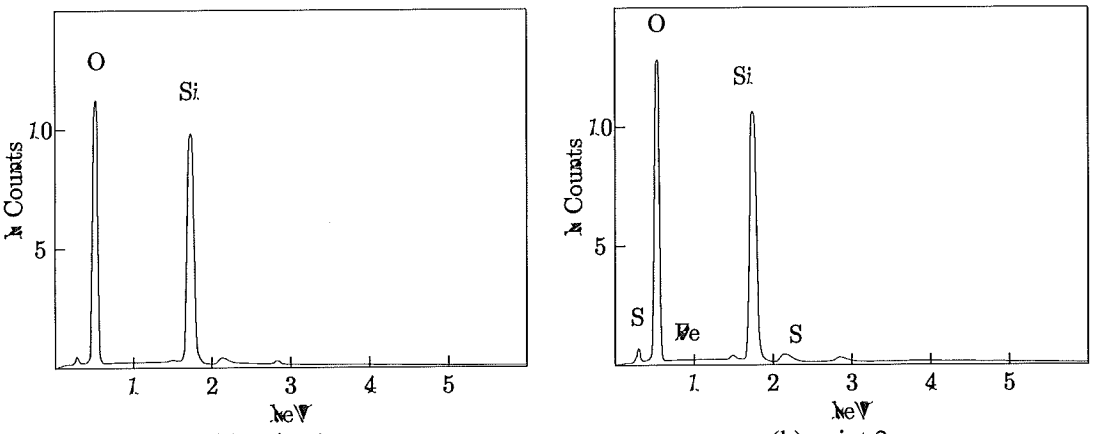

(a) point 1 (b) point 2

Fig. 7.9 EDS spectrum – aggregate

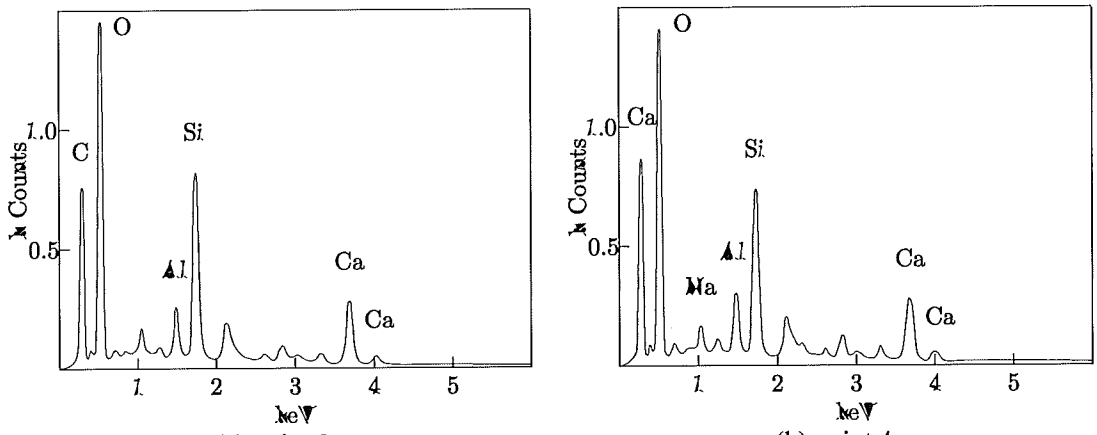

(a) point 3 (b) point 4

Fig. 7.10 EDS spectrum of matrix

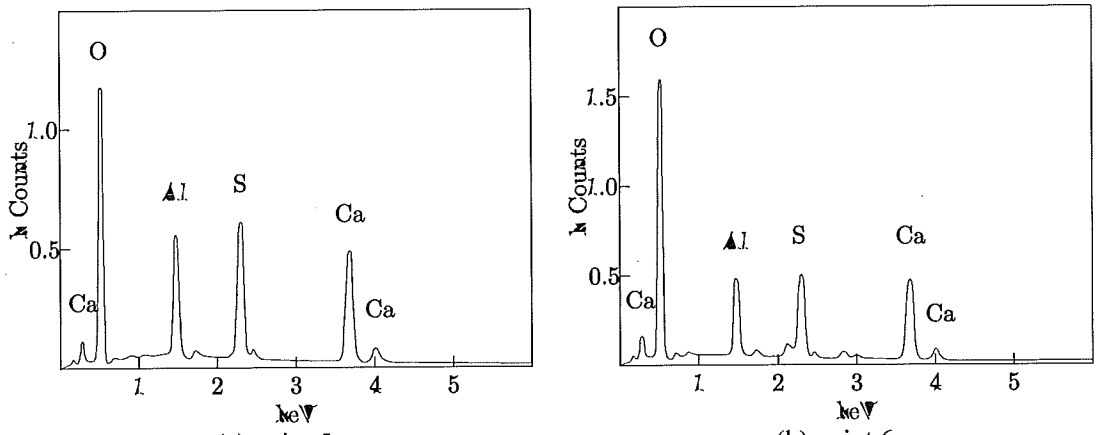

(a) point 5 (b) point 6

Fig. 7.11 EDS spectrum of secondary mineral - ettringite

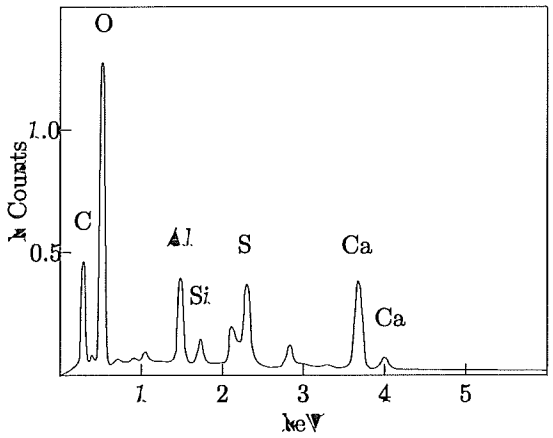

Fig. 7.12 EDS spectrum of point 6 - thaumasite

7.4.2 LARGE VOIDS IN MATRIX

Needle like secondary minerals were observed filling the large voids in the matrix as shown in **Fig. 7.13**. The dark grey phase is quartz aggregate as proven by the EDX analysis of two representative points (**Fig. 7.14**). Filling voids by secondary minerals is often associated with cracking (**Fig. 7.15a**). These cracks are either radially oriented micro cracks or propagate into the cement matrix. EDX analysis indicates that these secondary minerals are a mix of ettringite and thaumasite. The source of sulfate required for the formation of theses minerals may be due to the oxidation of pyrrhotite included in the aggregate. More ettringite is observed in the voids of matrix near aggregates that contain pyrrhotite inclusions than occurs near aggregate without pyrrhotite (**APPENDIX G**). Pyrrhotite in aggregate adjacent to open spaces, such as voids in matrix or the porous ITZ, have easier access to oxygen and water thus higher change of oxidization leading to higher concentration of secondary minerals in these areas.

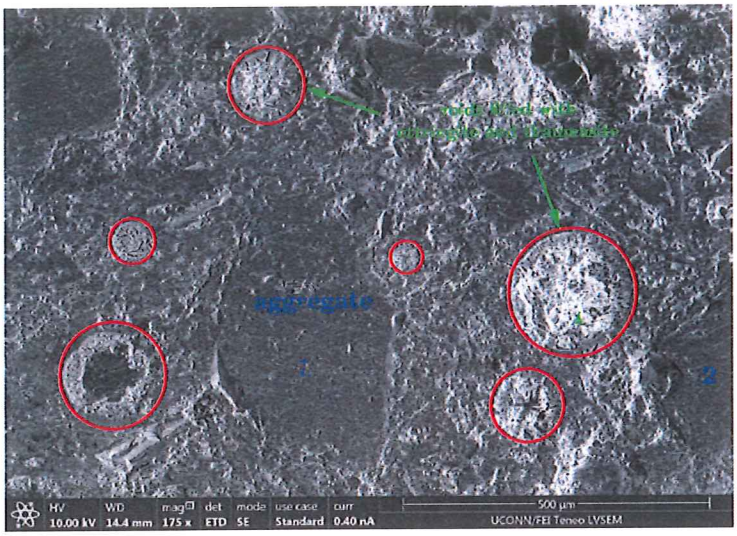

Fig. 7.13 Distribution of secondary minerals

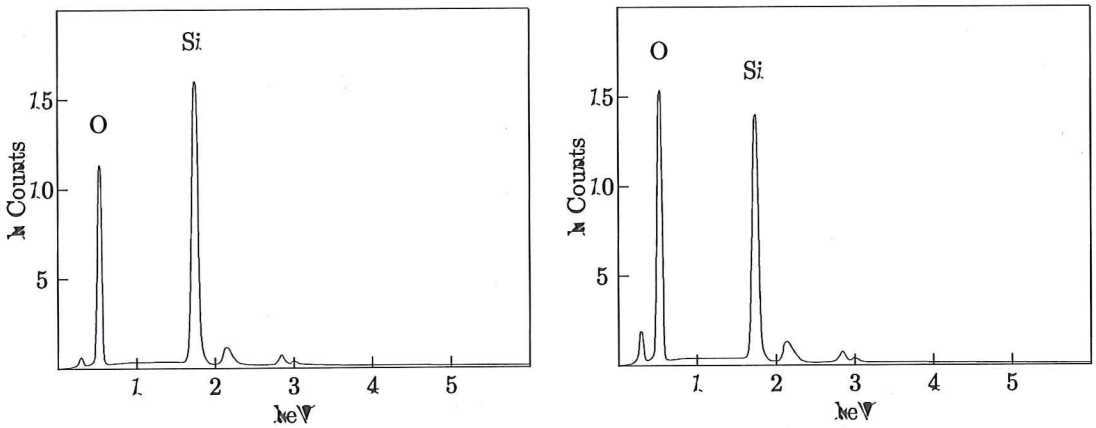

(a) point 1 (b) point 2

Fig. 7.14 EDX result for aggregate

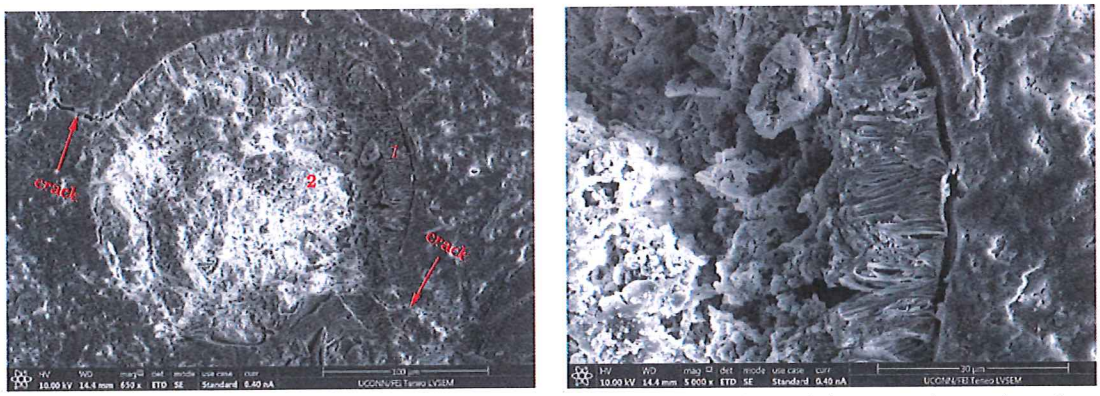

(a) cracked void filled with secondary minerals (b) close up view of the secondary minerals

Fig. 7.15 Secondary minerals deposited in the large voids of matrix

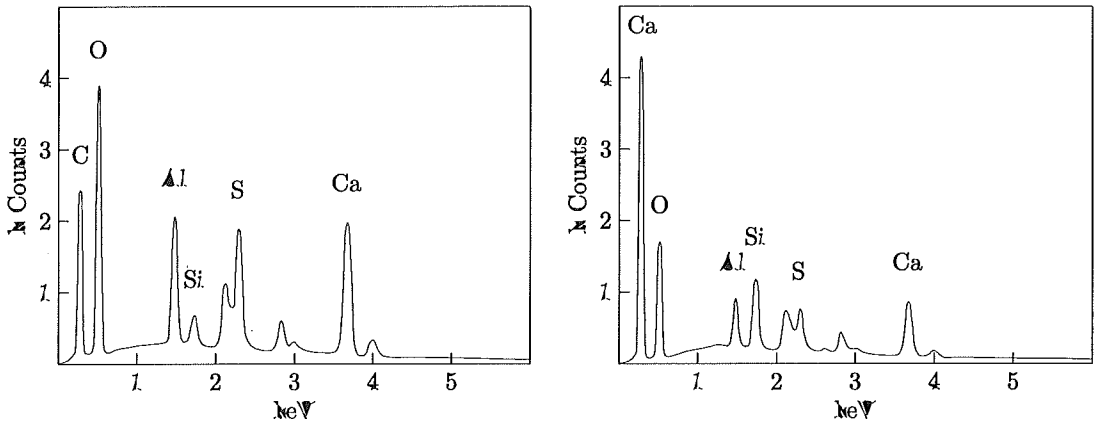

(a) thaumasite (b) ettringite

Fig. 7.16 EDX result for the minerals in void A

8. SUMMARY, CONCLUSIONS AND FUTURE EFFORTS

8.1 SUMMARY AND CONCLUSIONS

Based on the mechanical, mineralogical, microstructural and chemical tests on the core samples taken from 7 houses and the visual inspection of 14 additional houses, the primary findings are summarized as follows:

- Aggregates are rich in pyrrhotite ($Fe_{1-x}S$) and in their oxidization product such as goethite (FeO(OH)), ferrihydrite ($Fe(OH)_3$) and sulfur (S).
- The whitish deposits at the vicinity of cracking surface is primarily sulfate containing minerals such as thenardite (Na_2SO_4) and aphthitalite ($(K,Na)_3Na(SO_4)_2$).
- The matrix is porous with a large quantity of voids and the ITZ is porous. Abundance of secondary minerals such as ettringite ($Ca_6Al_2(SO_4)_3(OH)_{12}\cdot 26H_2O$) and thaumasite ($Ca_3Si(OH)_6(CO_3)(SO_4)\cdot 12H_2O$) are present in these open spaces. Cracking is often associated with these open spaces and either within the voids or propagates into cement matrix.

A hypothesis is established: pyrrhotite in the aggregate oxidizes at the presence of water and oxidant (oxygen or ferric ions) which lead to the formation of expansive secondary mineral product such as ferrihydrite and the release of sulfate. The released sulfate promotes the reaction with aluminum containing phases in the cement (tricalcium aluminate ($3CaO\cdot Al_2O_3$)) and results in the formation of expansive and thus deleterious secondary minerals such as ettringite. Furthermore, at the presence of carbon, either from the calcite in aggregate or from CO_2 from environment, another deleterious mineral thaumasite can be formed. Both of these secondary minerals are expansive and might ultimately lead to the premature deterioration of the concrete foundation investigated in this research. The hypothesis is validated by the chemical, mineralogical and microstructural investigation on the pyrrhotite-bearing aggregate, sulfate

containing whitish deposits found at the vicinity of the cracking surface along with the spatial association of secondary minerals with microcracks in the cement matrix.

8.2 FUTURE EFFORTS

Understanding the cause of the early deterioration of concrete foundation walls facilitates future efforts to address some potential concerns as follows:

- What percentage of pyrrhotite contained in concrete aggregate can cause premature deterioration?

  This will require reproducing deterioration processes under isolated conditions in the laboratory, tailoring laboratory experiments and test protocols, and coupling of macro- and micro- analysis.

- What methods and investigations are suggested to determine the stage of deterioration?

  This will require finding effective test methods and providing recommendations for homeowners and contractors.

- What solutions can be found to reduce and mitigate the pyrrhotite-based deterioration of concrete?

  This will require finding mechanical or chemical solutions or a combination of both to address the stage- dependent deterioration.

- Can solutions be found to allow the use of pyrrhotite containing aggregates in concrete mixes for particular purposes?

  This will require isolated investigation of mixture design parameters.

APPENDICES

APPENDIX A: PHOTOS OF THE DETERIORATION OF THE INSPECTED HOUSES

(a) whitish powder

(b) brown trace

(c) map cracking

(d) wide crack opening

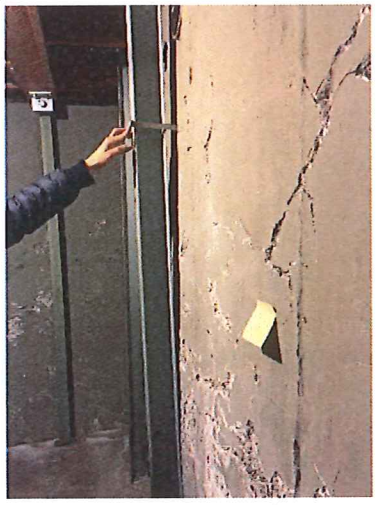

(e) large deformation

Fig. A- 1 House 1

(a) whitish powder

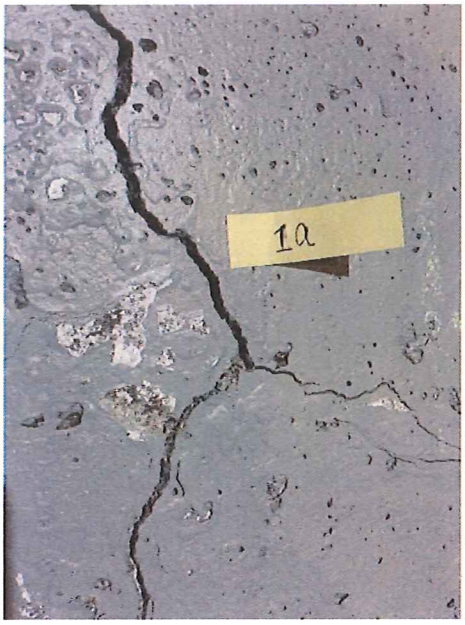

(b) brown trace

(c) wide crack opening

Fig. A- 2 House 2

(a) whitish powder

(b) brown trace

(c) map cracking

(d) wide crack opening

Fig. A- 3 House 3

(a) whitish powder

(b) brown trace

(c) map cracking

(d) wide crack opening

Fig. A- 4 House 4

(a) whitish powder

(c) map cracking

(d) wide crack opening

Fig. A- 5 House 5

(a) whitish powder

(b) map cracking

(c) wide crack opening

Fig. A- 6 House 6

(a) whitish powder (b) map cracking

Fig. A- 7 House 7

APPENDIX B: SEM-EDX TEST FOR QUARRY AGGREGATE

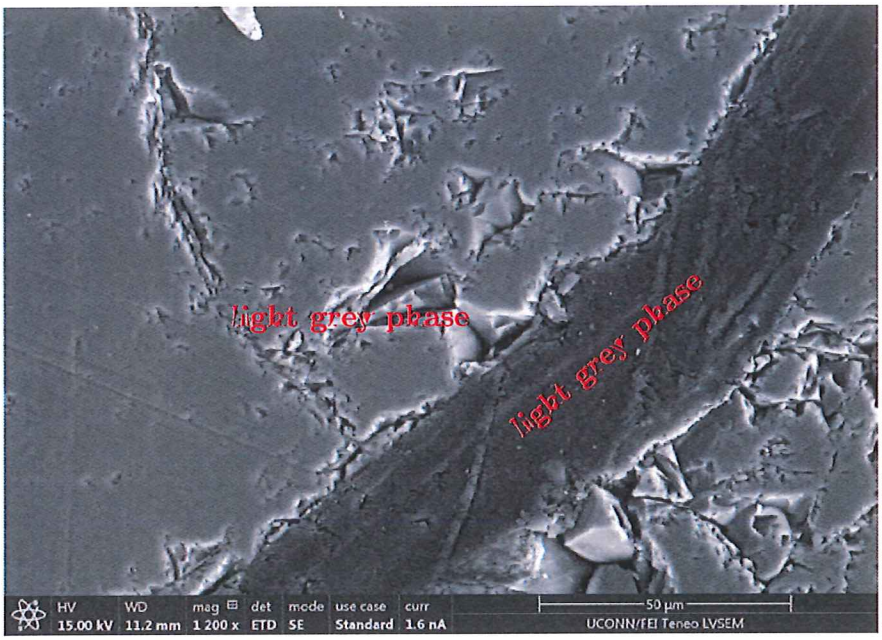

Fig. B- 1 SEM images of the coarse quarry aggregate – Sample 2

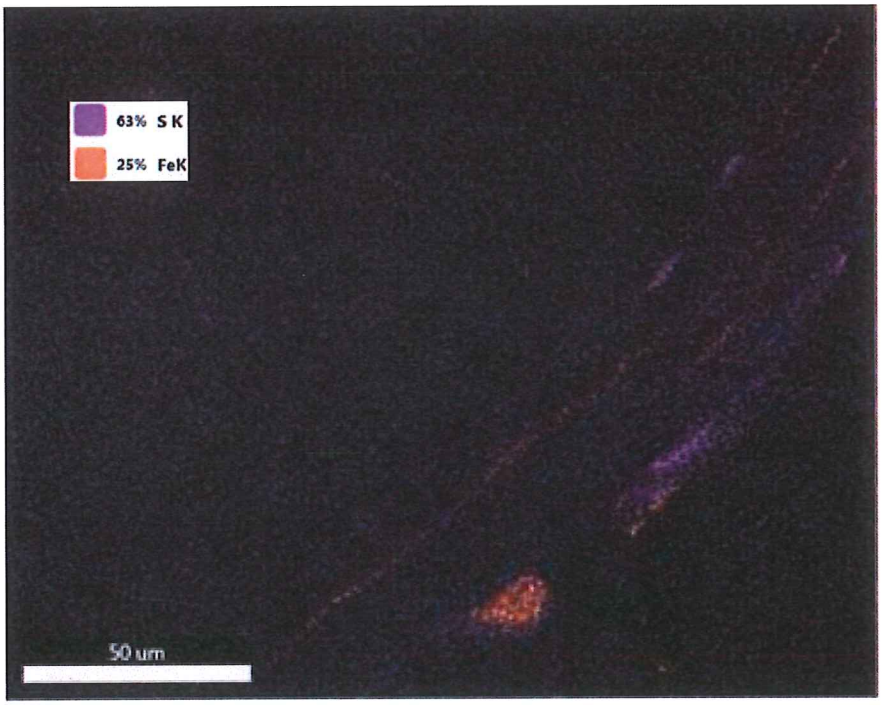

Fig. B- 2 EDX mapping elementary analysis for the interface zone – sample 2

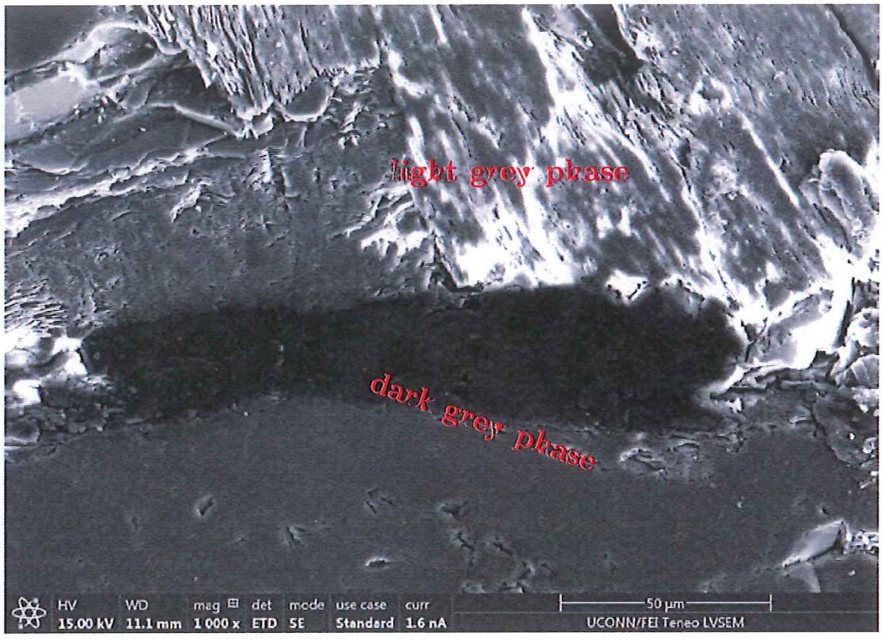

Fig. B- 3 SEM images of the coarse quarry aggregate – Sample 3

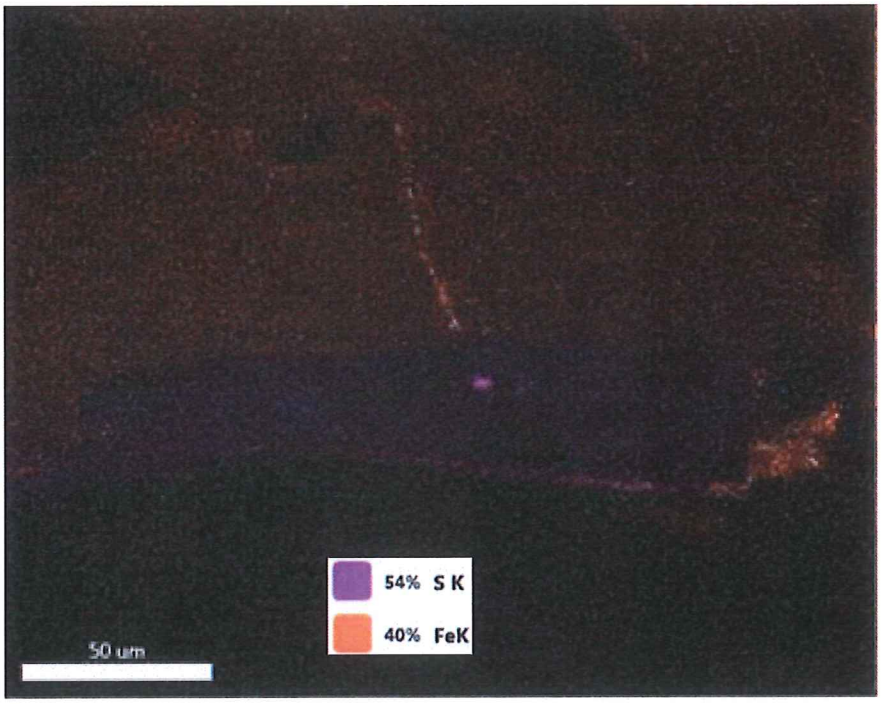

Fig. B- 4 EDX mapping elementary analysis for the interface zone – sample 3

APPENDIX C: XRD TEST FOR AGGREGATES FROM DETERIORATED CORE SAMPLES

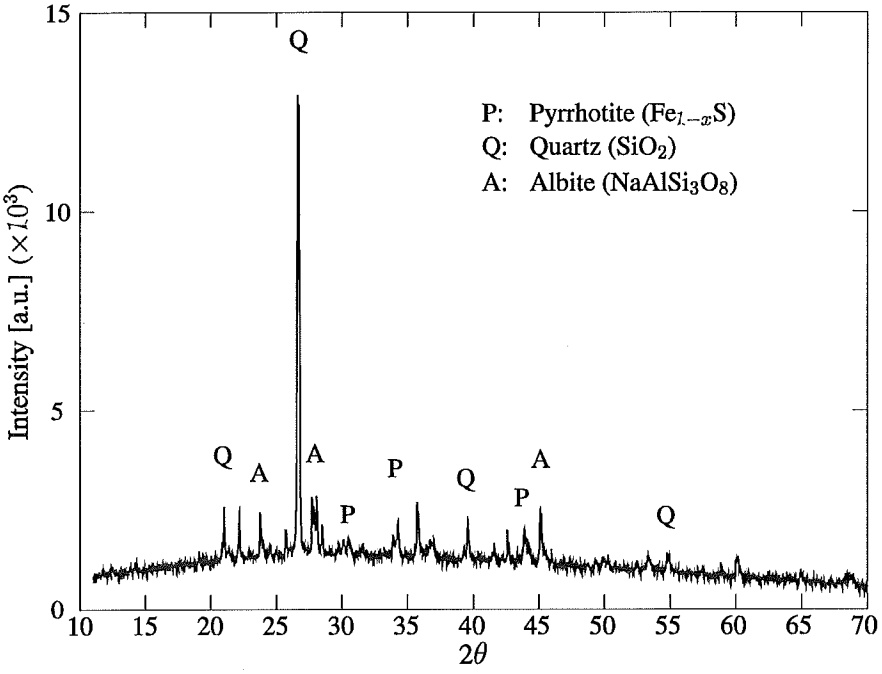

Fig. C- 1 House 1 Sample 1

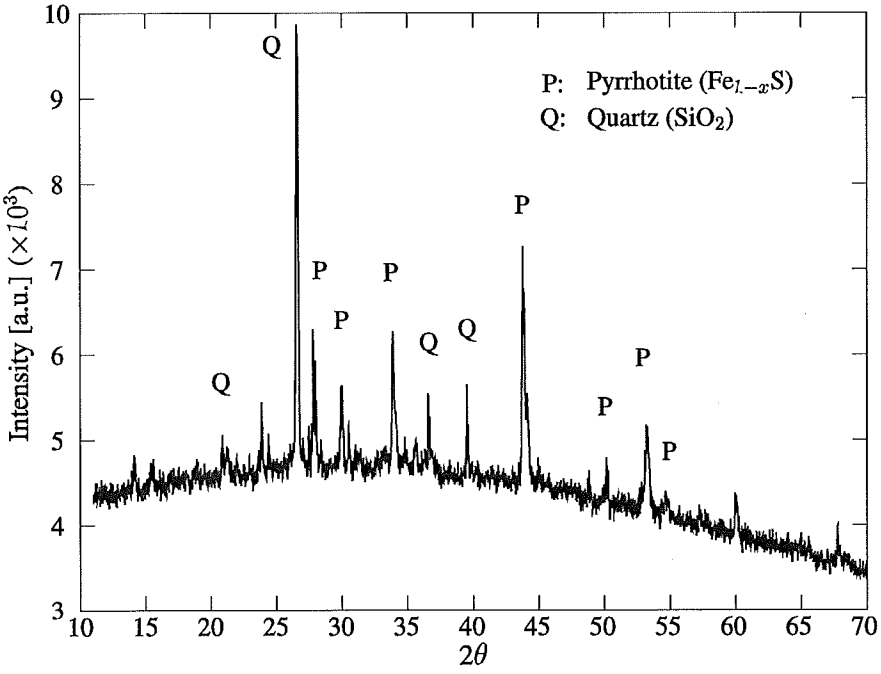

Fig. C- 2 House 1 Sample 2

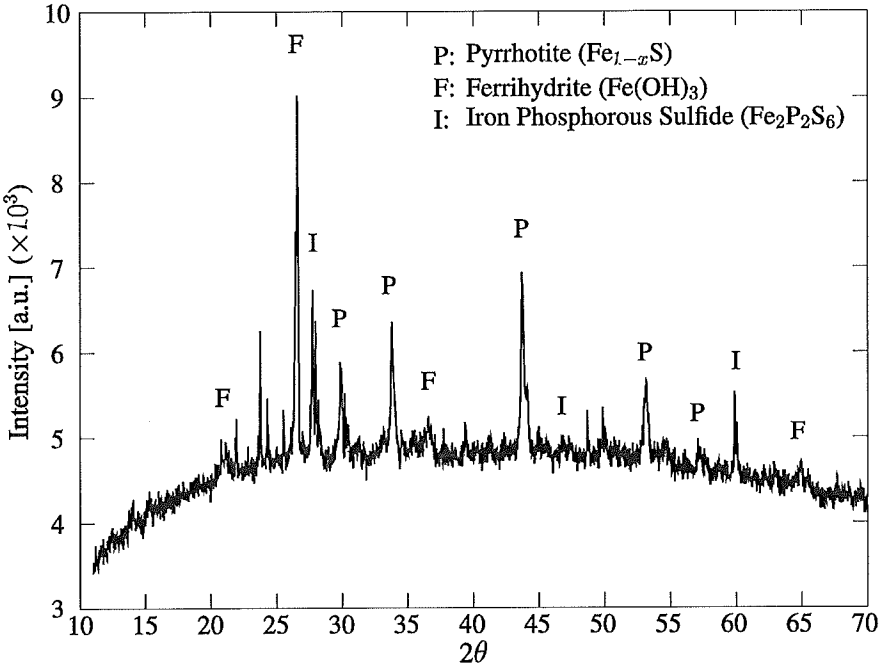

Fig. C- 3 House 2 Sample 1

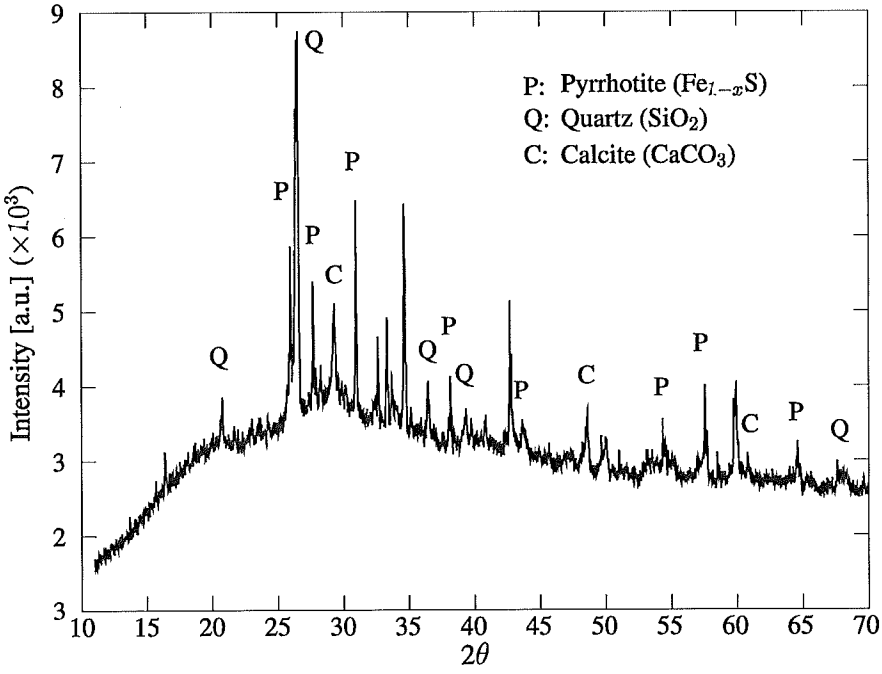

Fig. C- 4 House 2 Sample 2

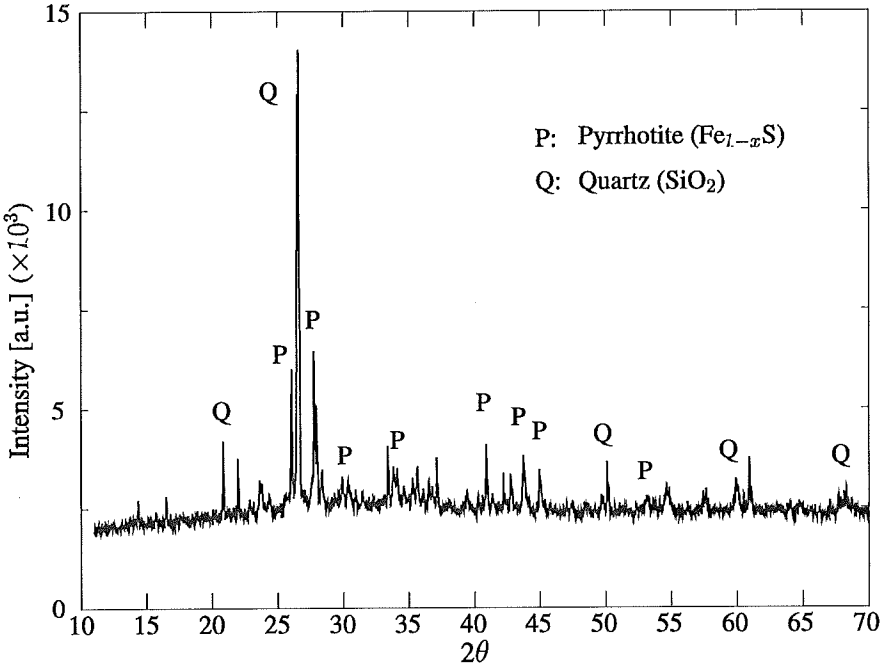

Fig. C- 5 House 3 Sample 1

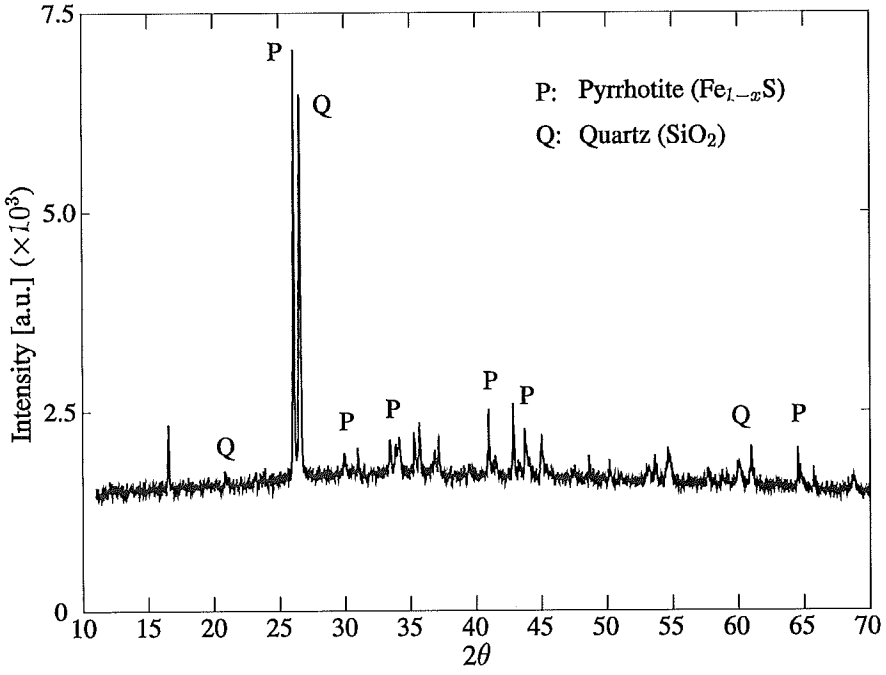

Fig. C- 6 House 3 Sample 2

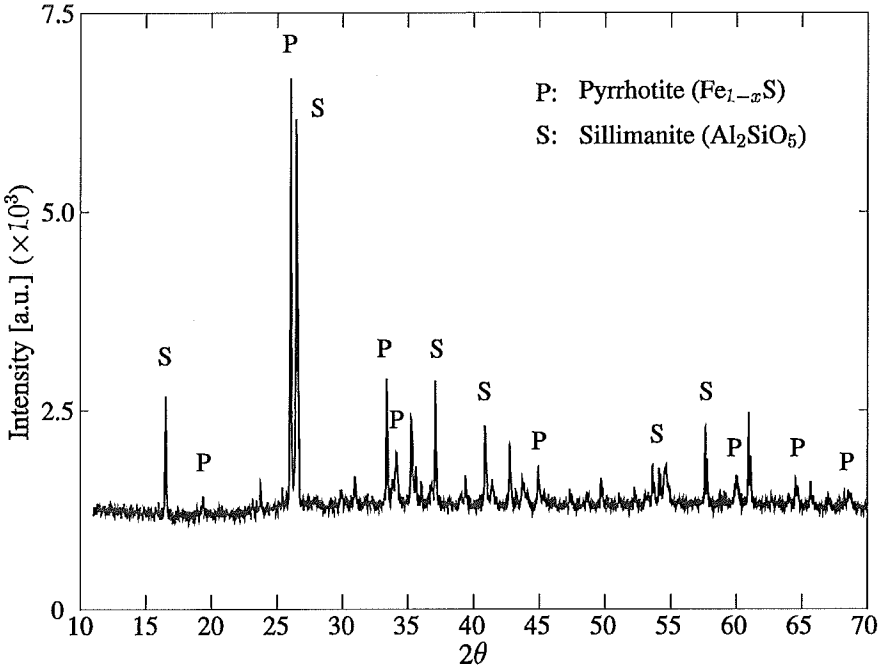

Fig. C- 7 House 3 Sample 3

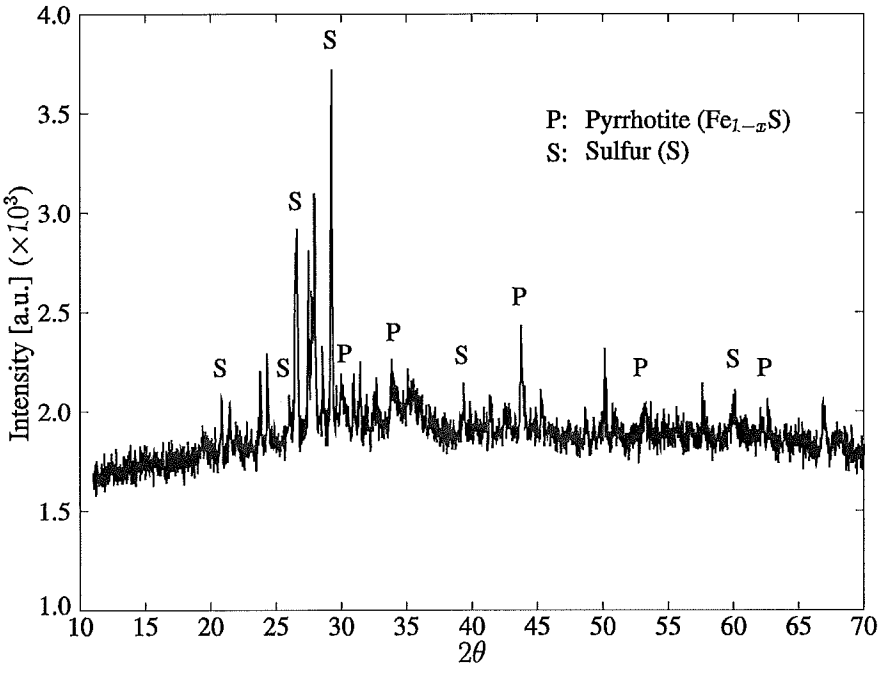

Fig. C- 8 House 4 Sample 1

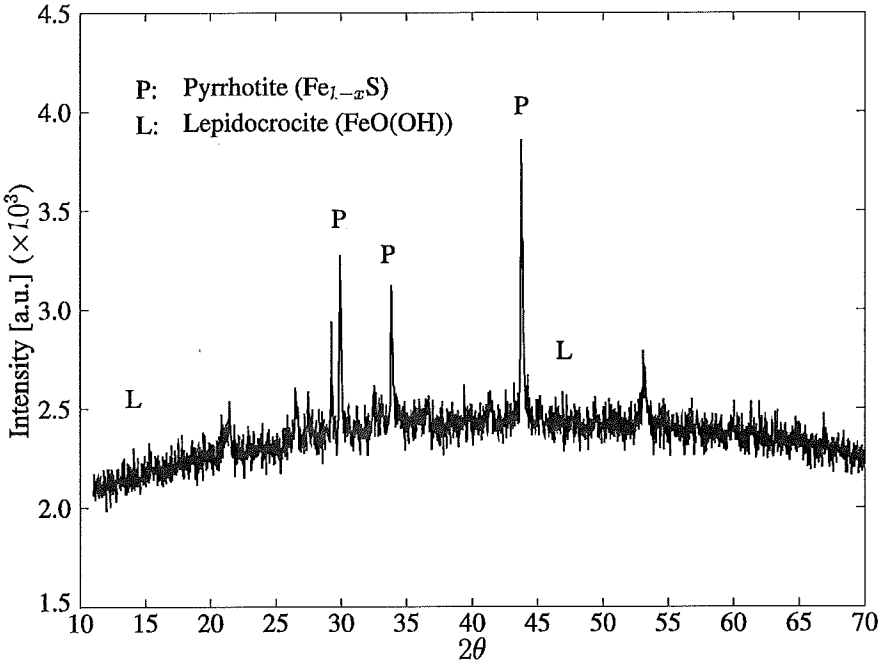

Fig. C- 9 House 4 Sample 2

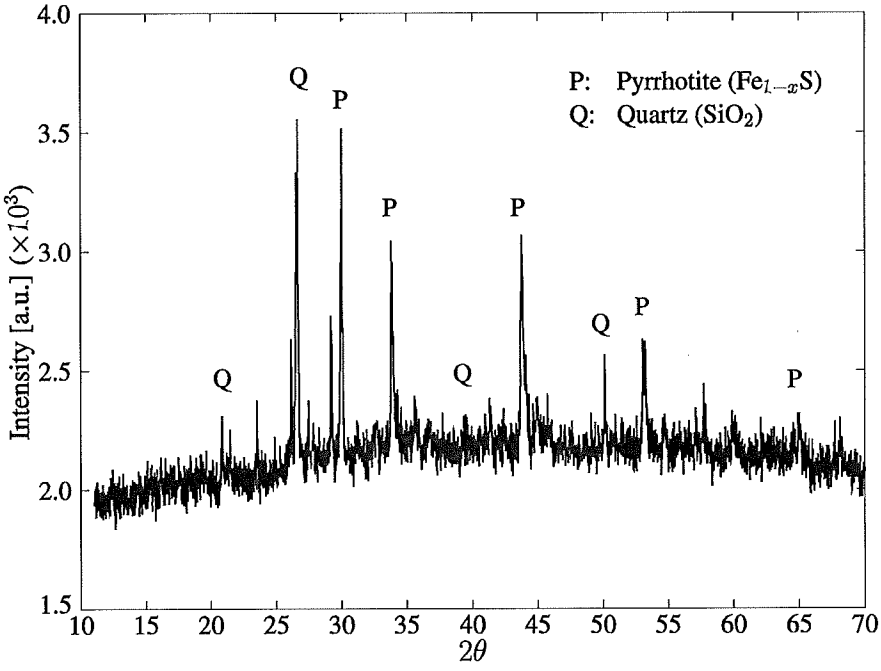

Fig. C- 10 House 4 Sample 3

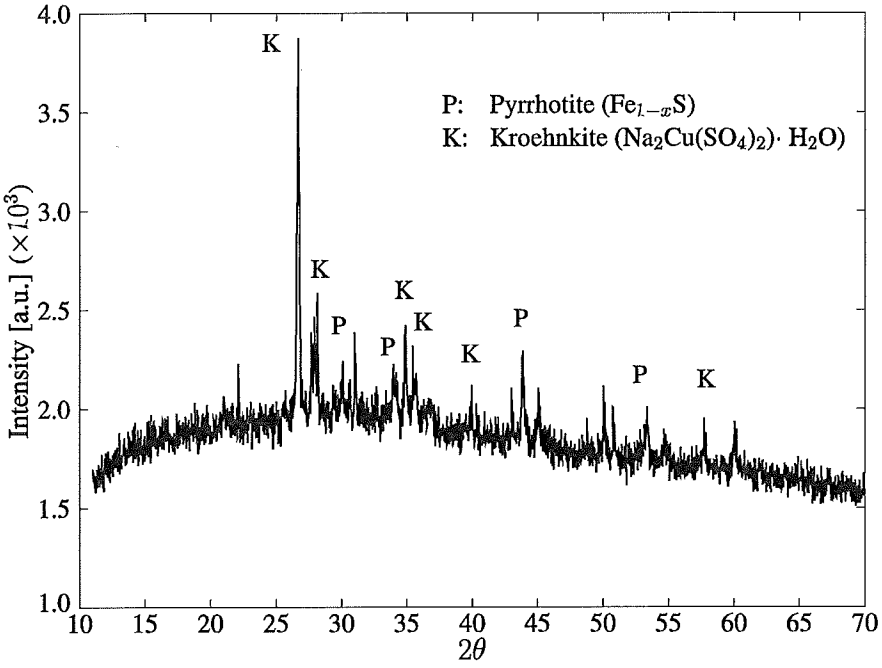

Fig. C- 11 House 5 Sample 1

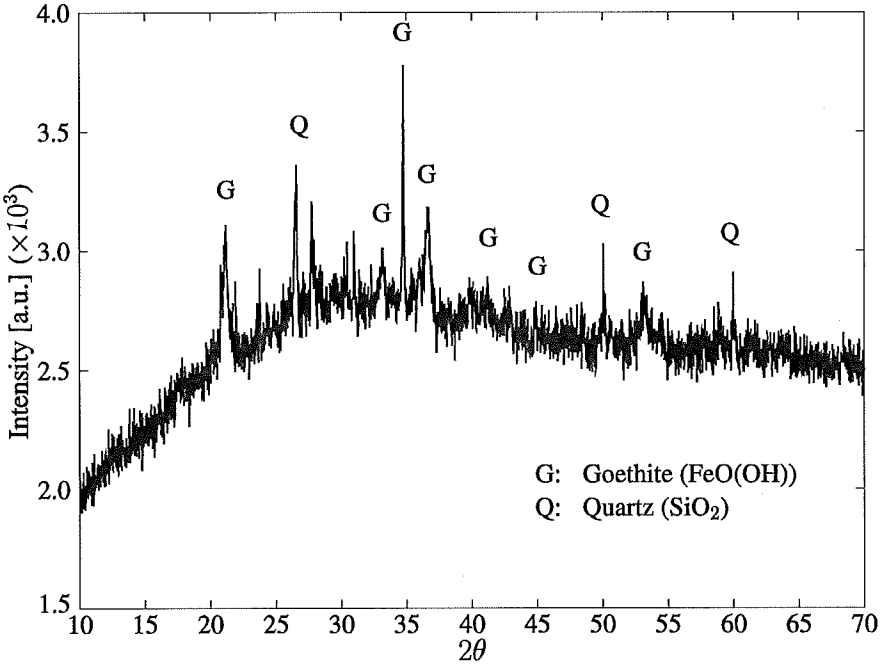

Fig. C- 12 House 5 Sample 2

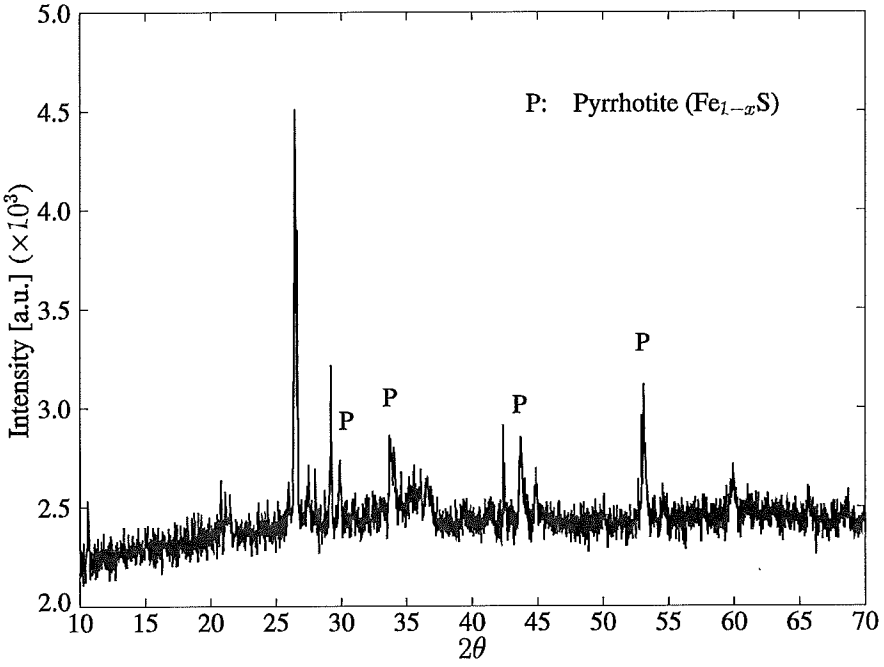

Fig. C- 13 House 5 Sample 3

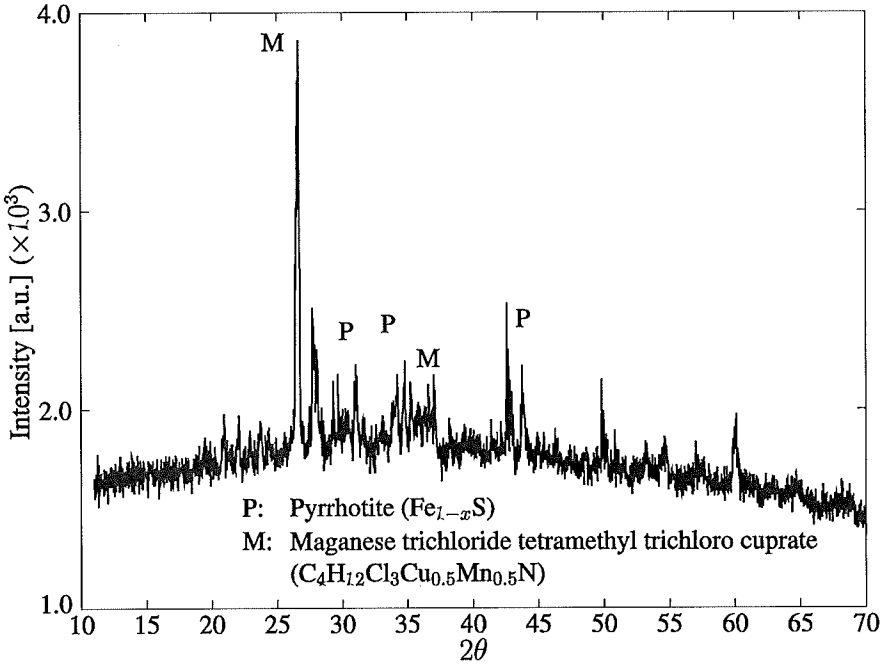

Fig. C- 14 House 6 Sample 1

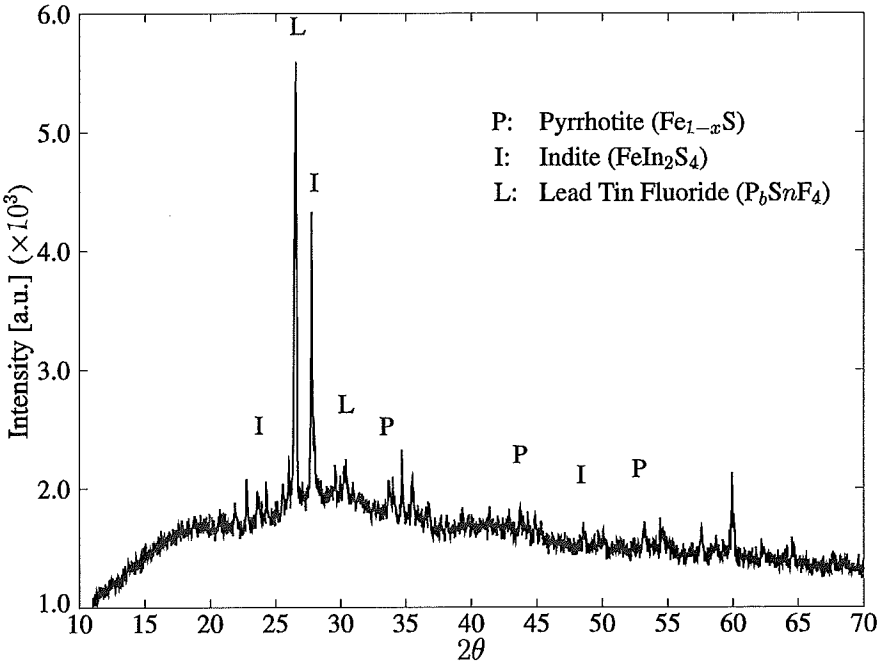

Fig. C- 15 House 6 Sample 2

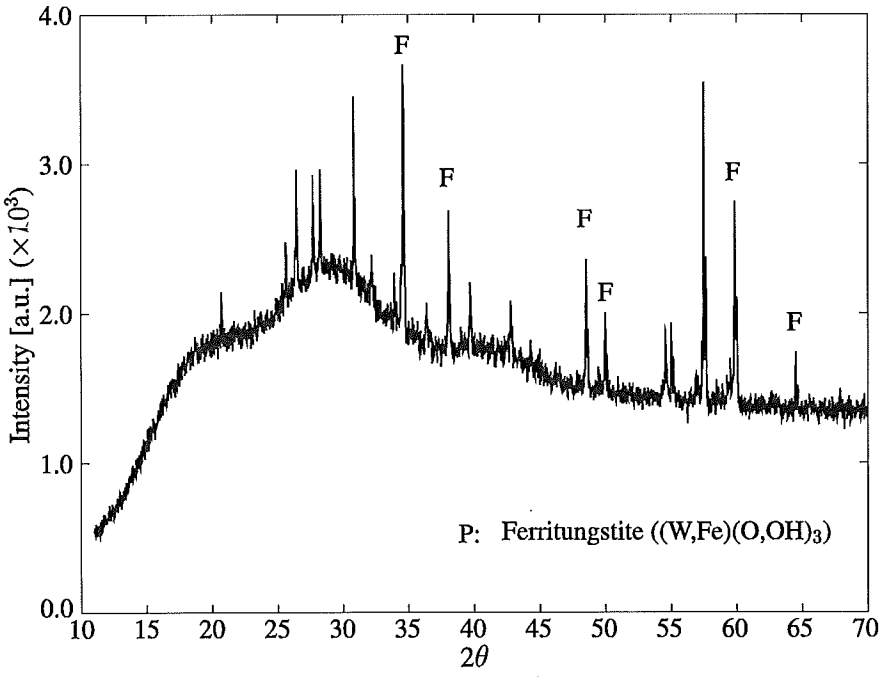

Fig. C- 16 House 7 Sample 1

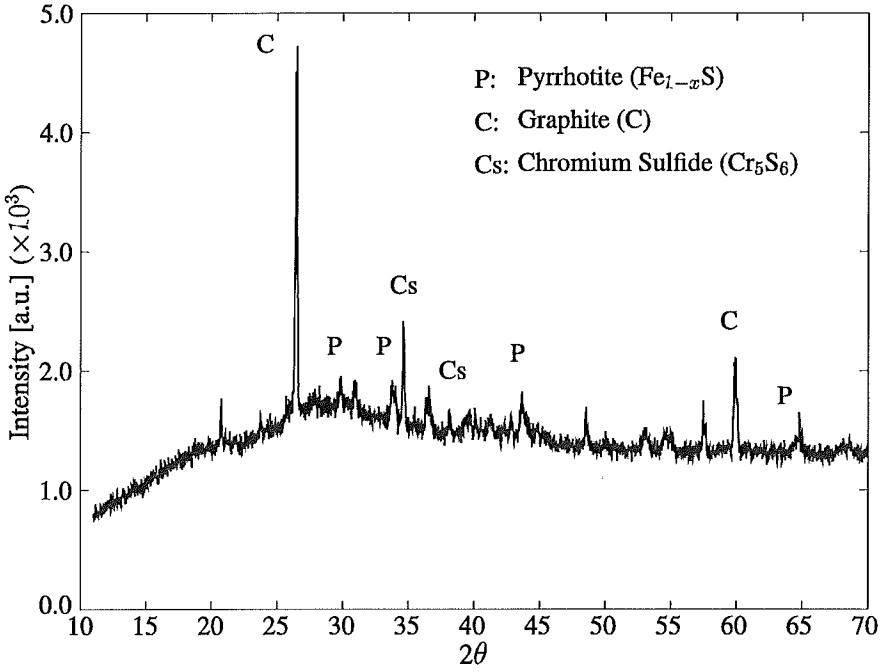

Fig. C- 17 House 7 Sample 2

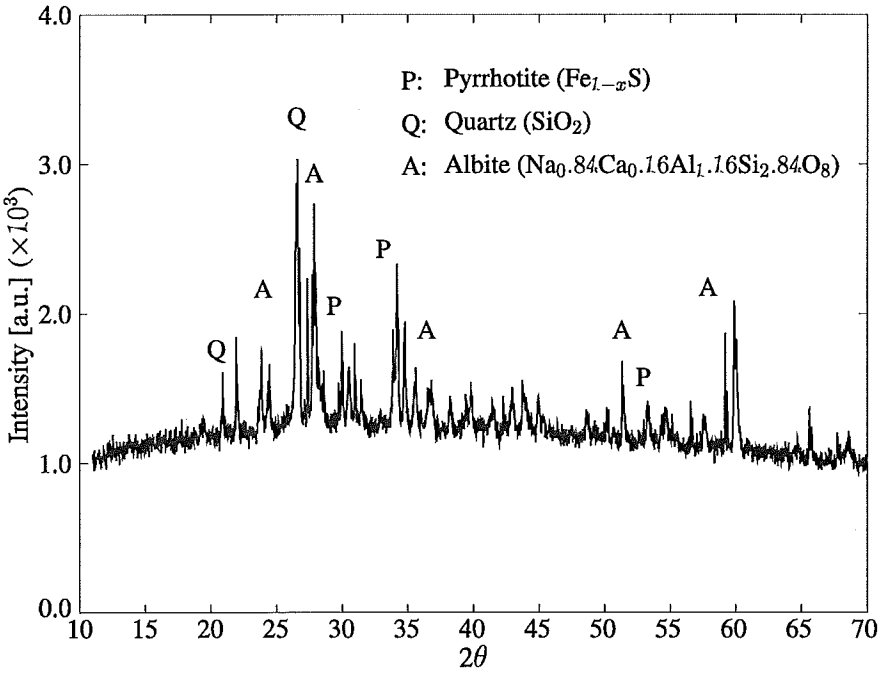

Fig. C- 18 House 7 Sample 3

APPENDIX D: XRD TEST FOR WHITISH POWDER

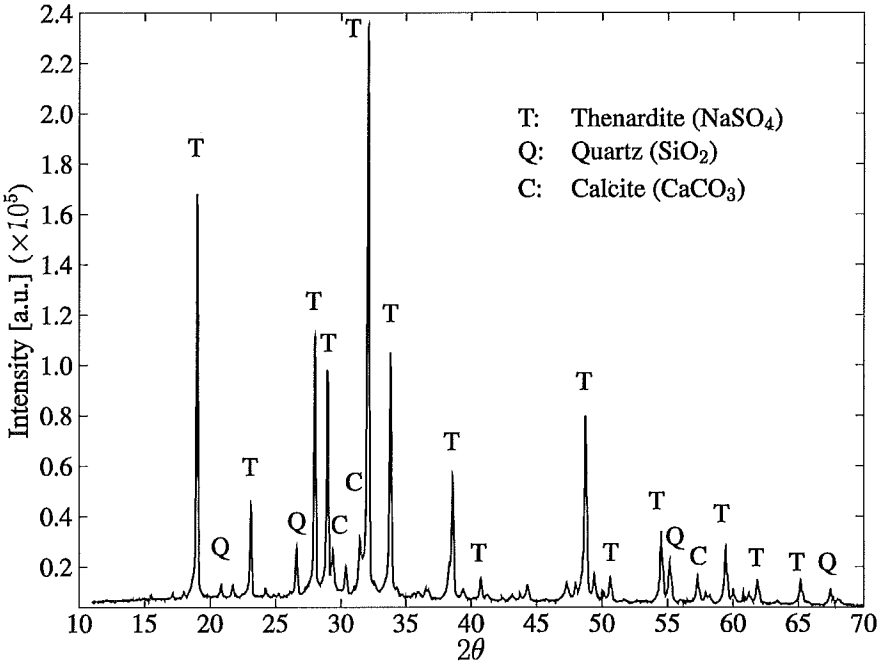

Fig. D- 1 House 1 Sample 1

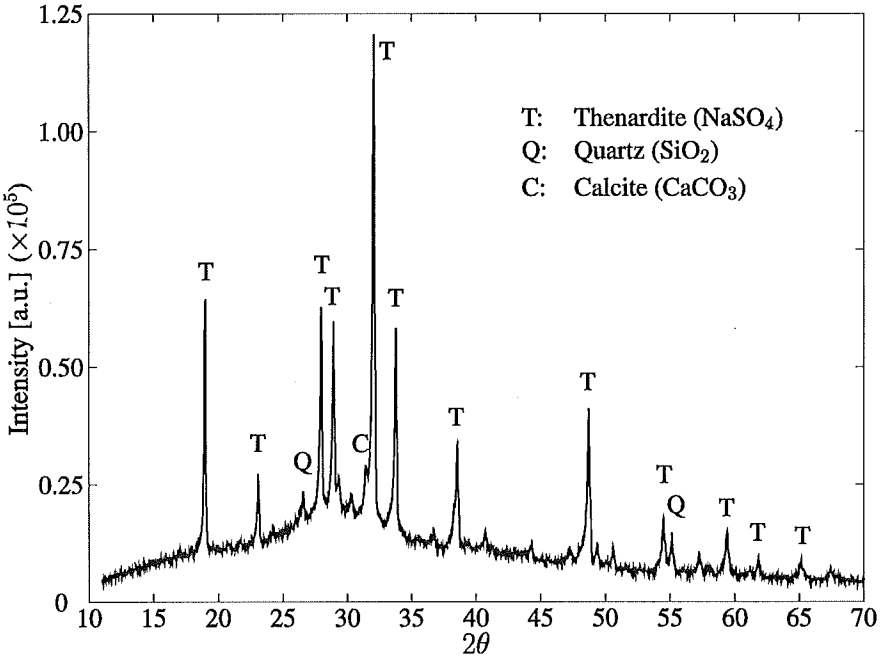

Fig. D- 2 House 1 Sample 2

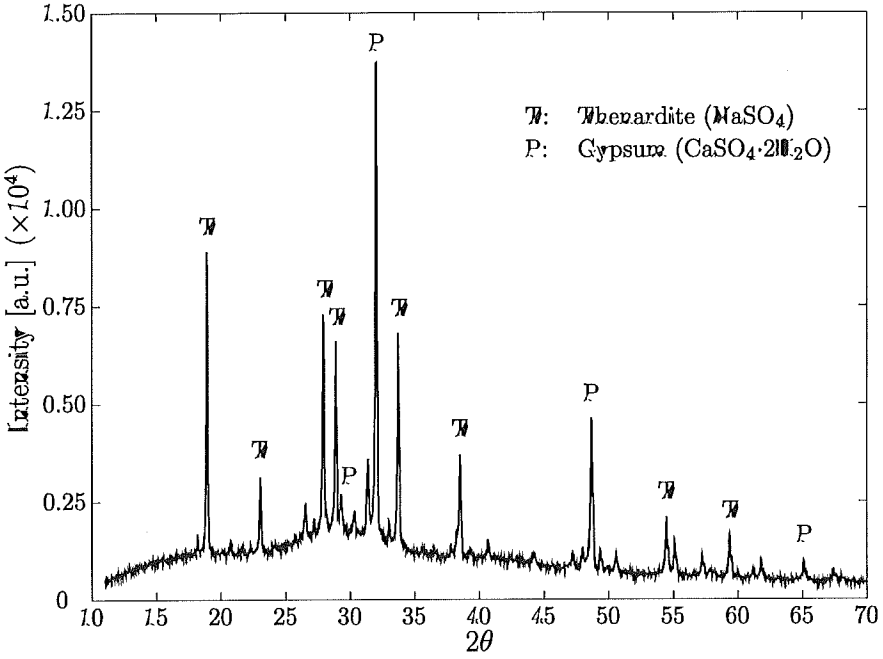

Fig. D- 3 House 1 Sample 3

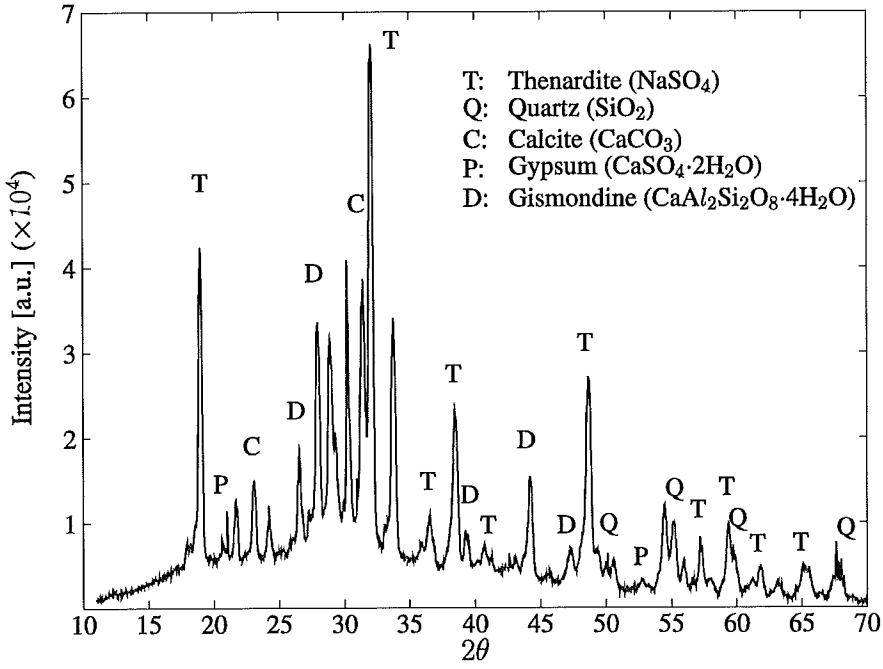

Fig. D- 4 House 2 Sample 1

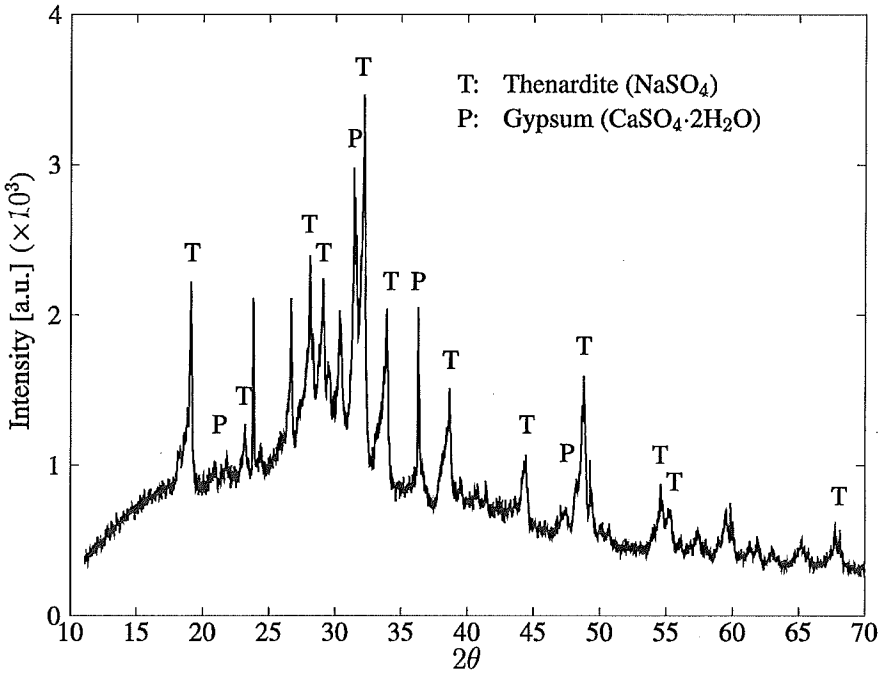

Fig. D- 5 House 2 Sample 2

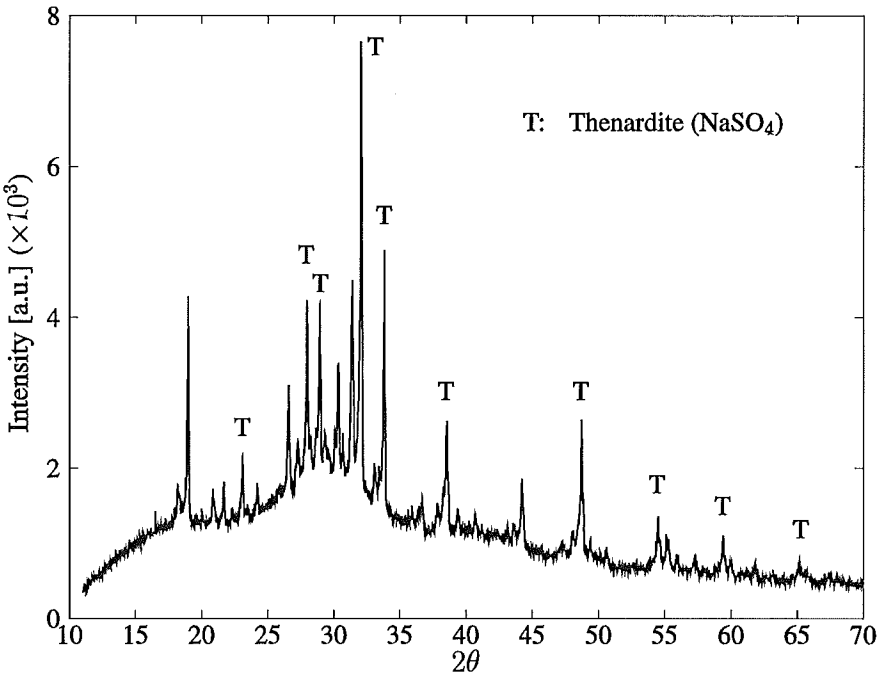

Fig. D- 6 House 2 Sample 3

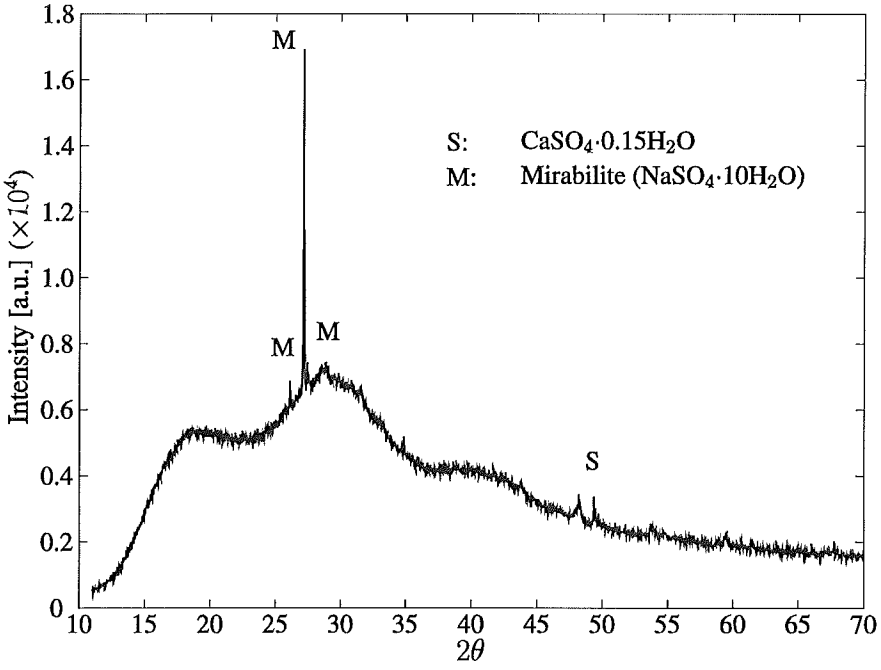

Fig. D- 7 House 3 Sample 1

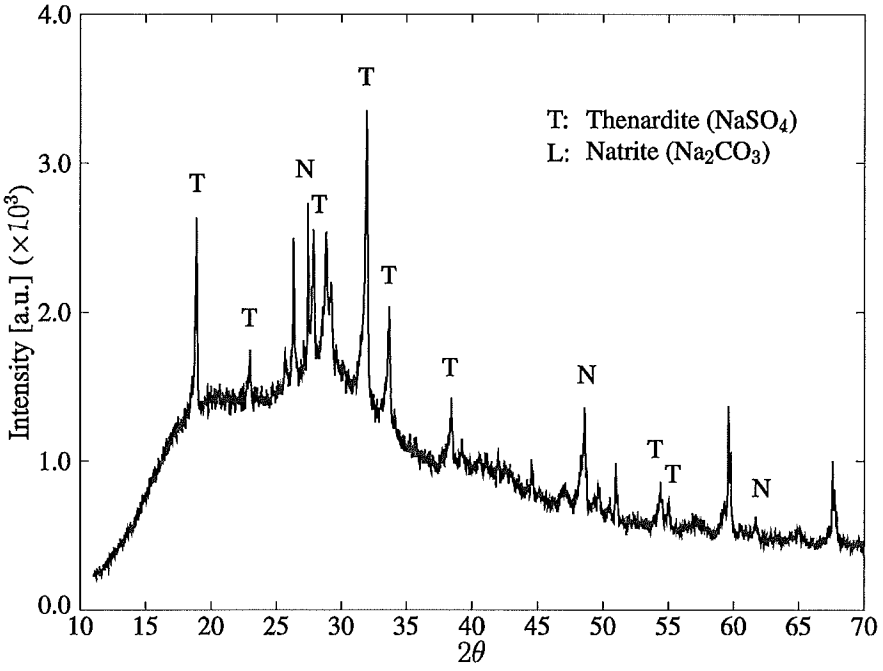

Fig. D- 8 House 4 Sample 1

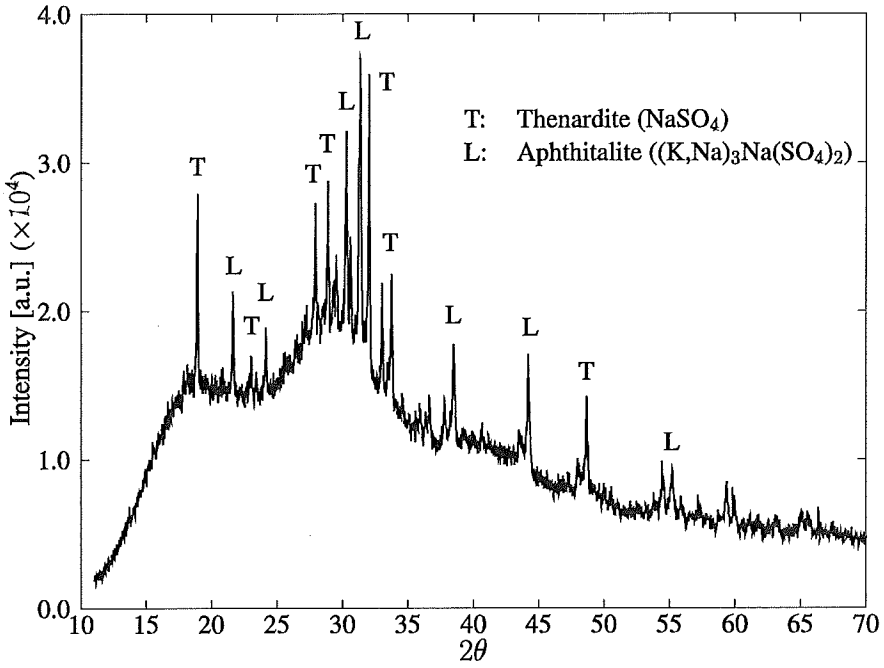

Fig. D- 9 House 5 Sample 1

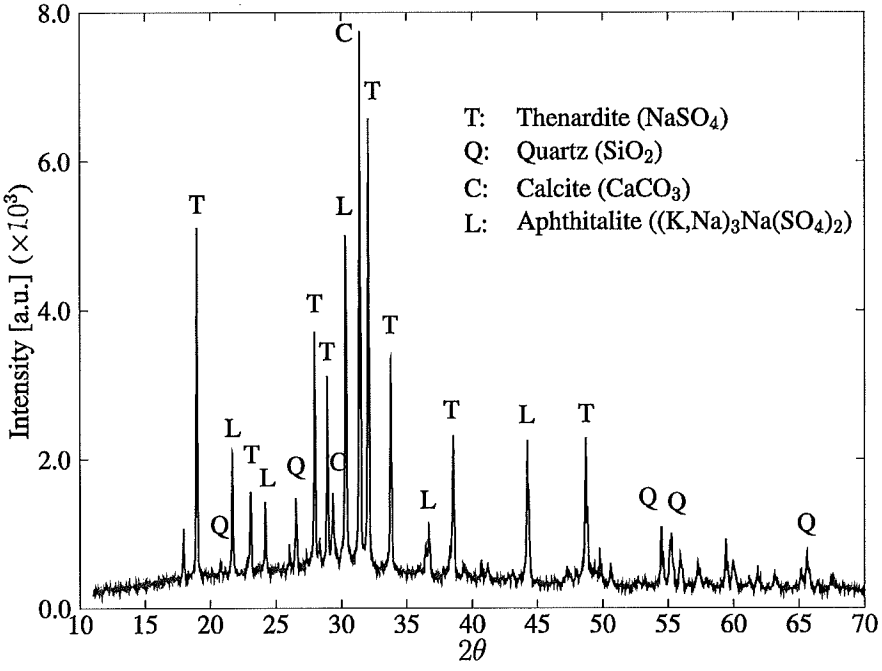

Fig. D- 10 House 5 Sample 2

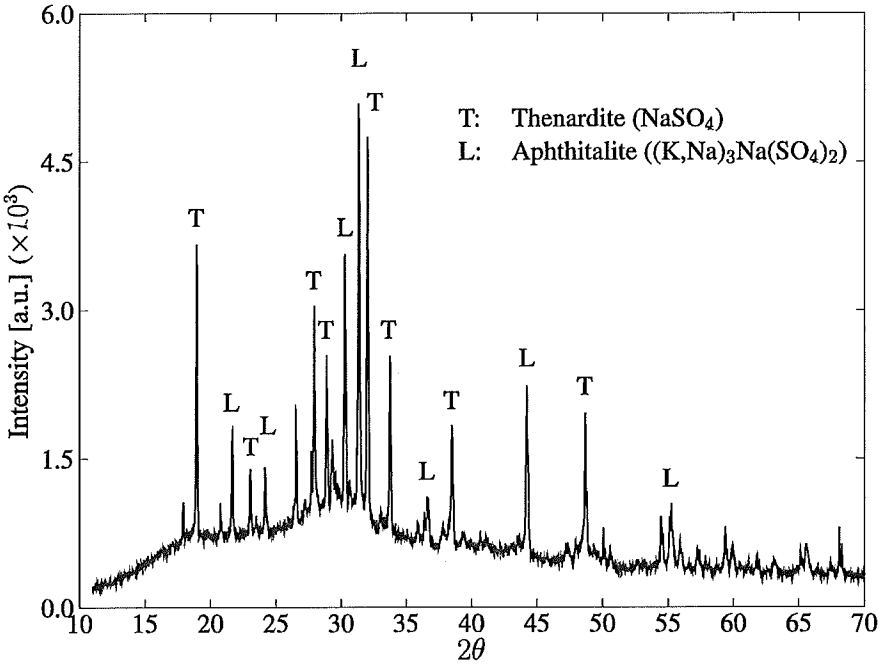

Fig. D- 11 House 5 Sample 3

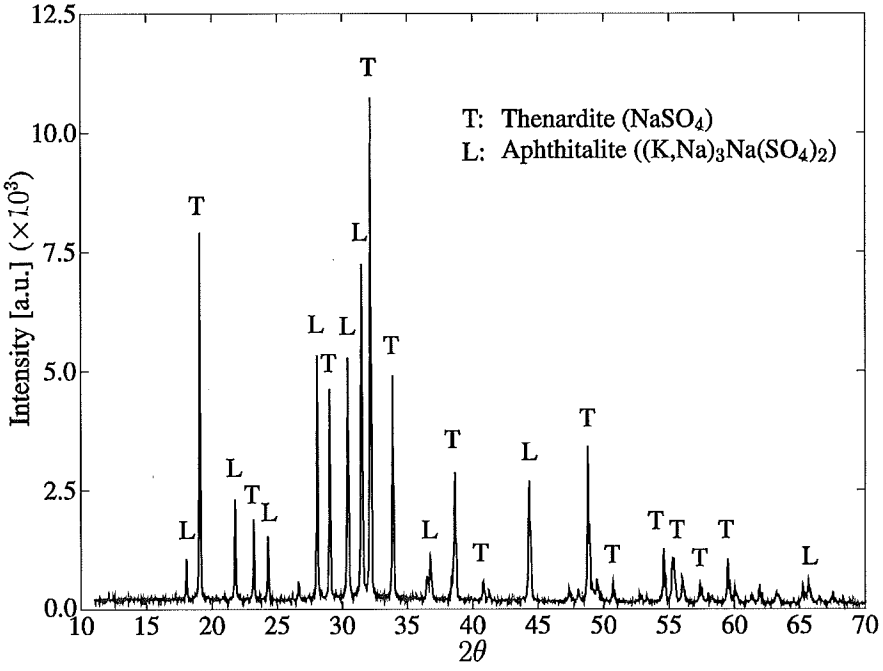

Fig. D- 12 House 7 Sample 1

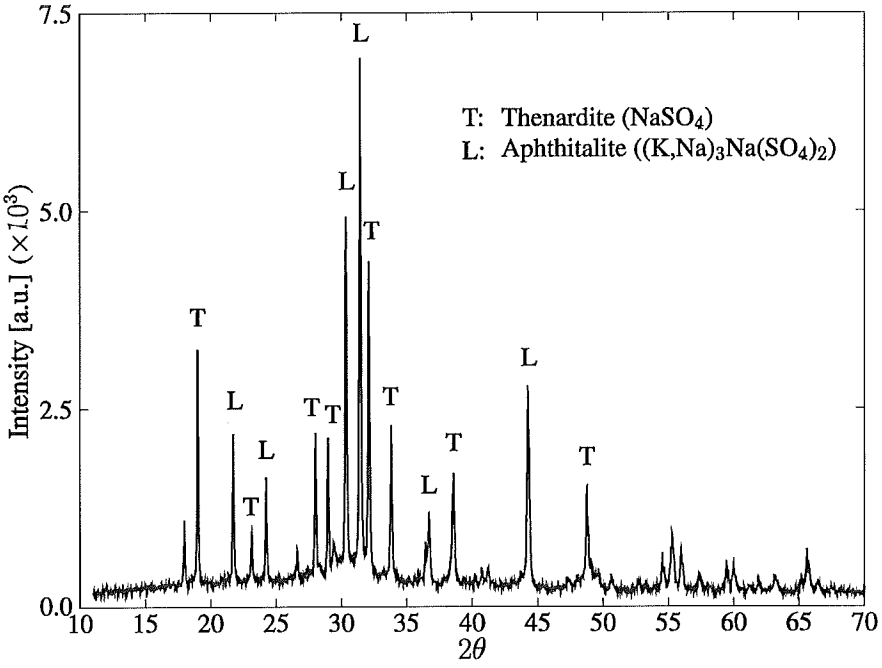

Fig. D- 13 House 7 Sample 2

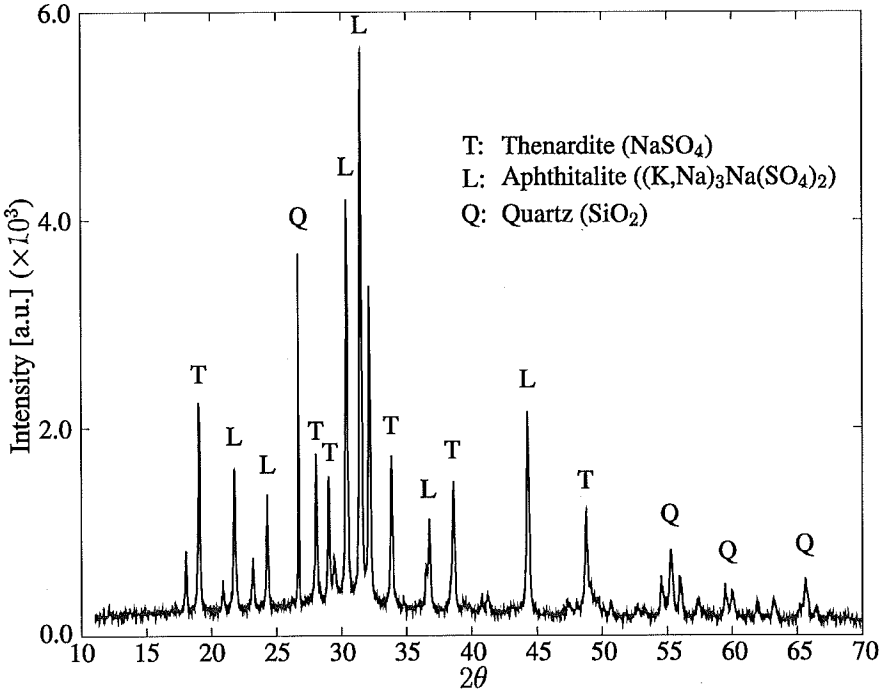

Fig. D- 14 House 3 Sample 3

APPENDIX E: PYRRHOTITE-BEARING AGGREGATE OXIDIZATION

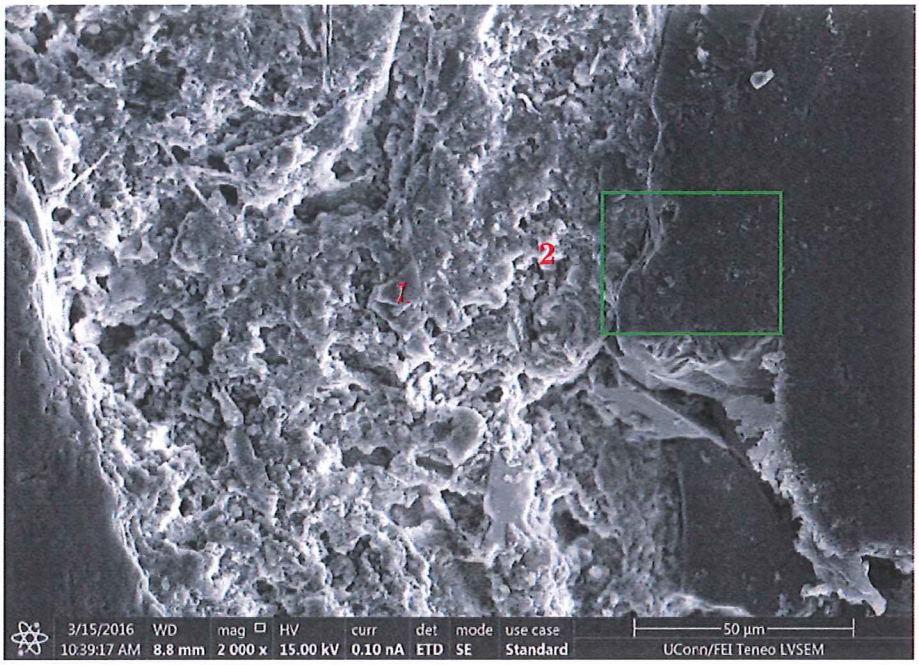

Fig. E- 1 Pyrrhotite-bearing aggregate

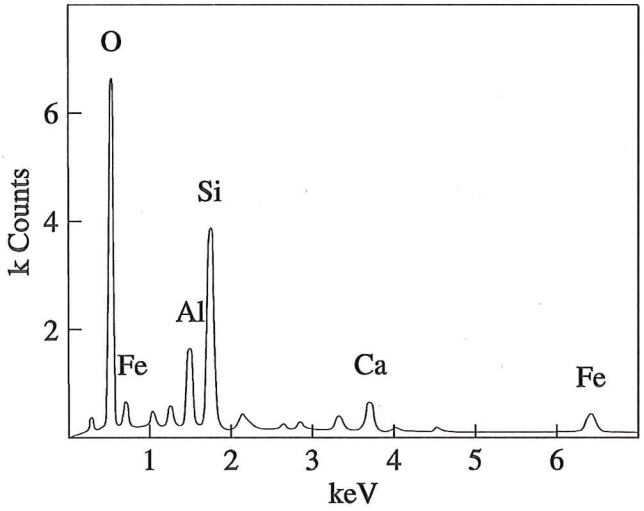

Fig. E- 2 DEX spectrum – point 1

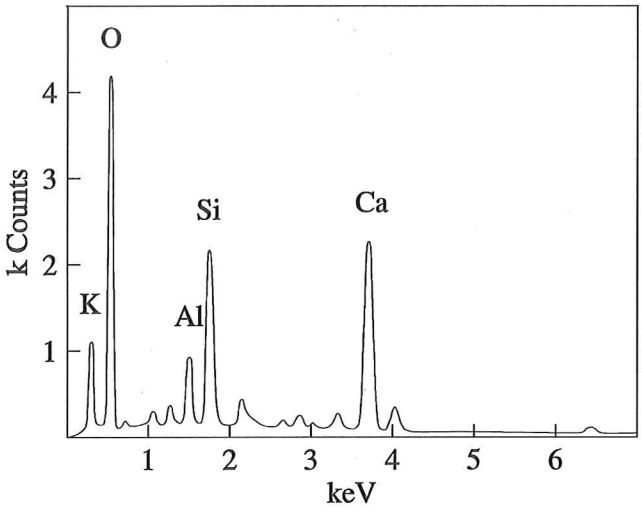

Fig. E- 3 DEX spectrum – point 2

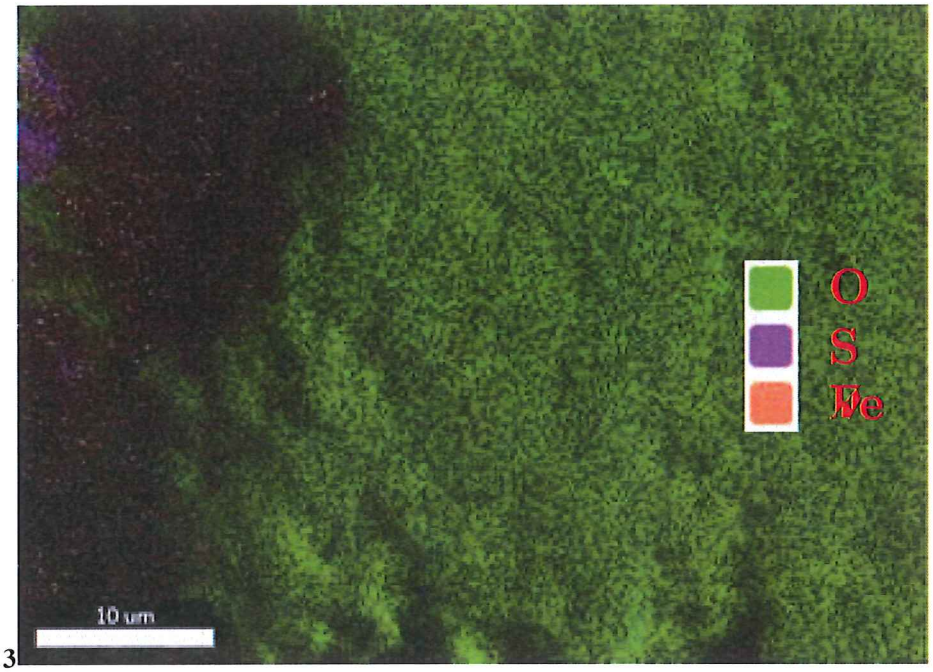

3

Fig. E- 4 EDS mapping analysis – Rectangular area in Fig. E- 1

APPENDIX F: SECONDARY MINERALS IN ITZ

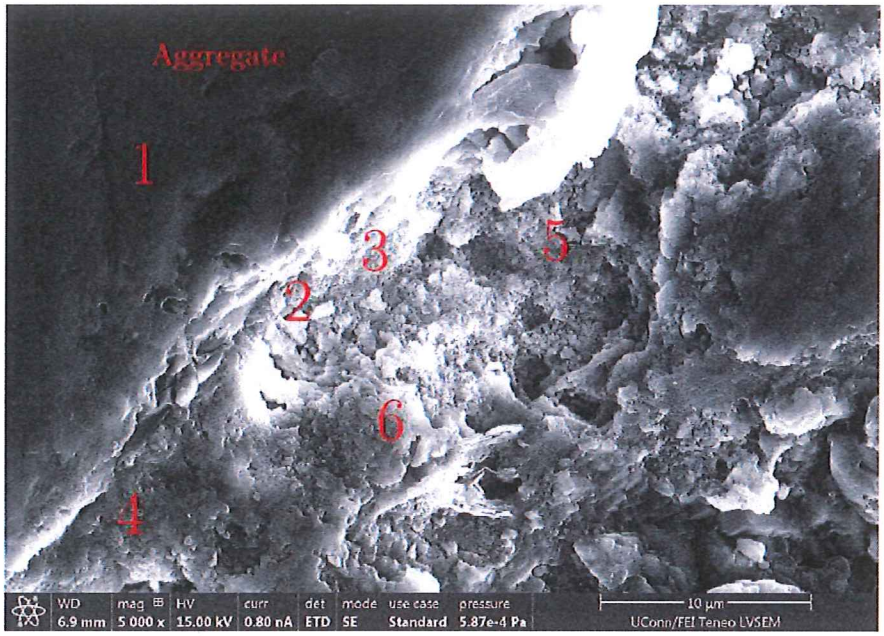

Fig. F- 1 Secondary minerals in the ITZ

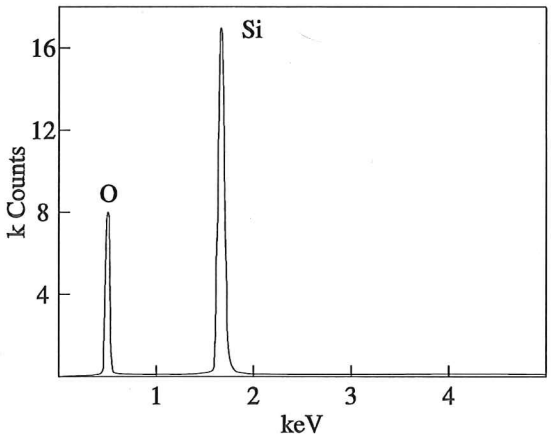

Fig. F- 2 EDS spectrum of point 1 – quartz aggregate

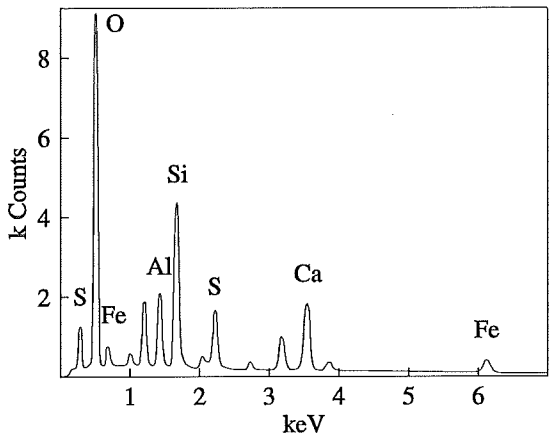

Fig. F- 3 EDS spectrum of point 2 – ettringite

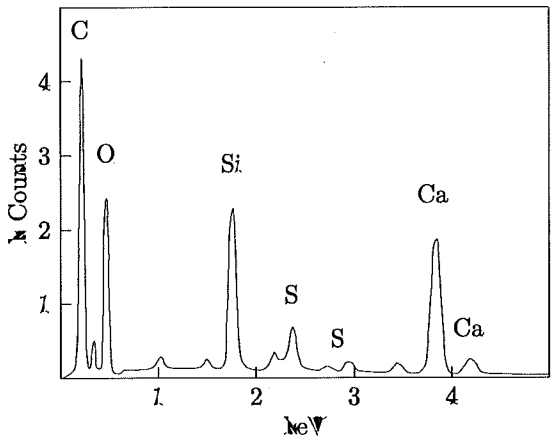

Fig. F- 4 EDS spectrum of point 3 matrix

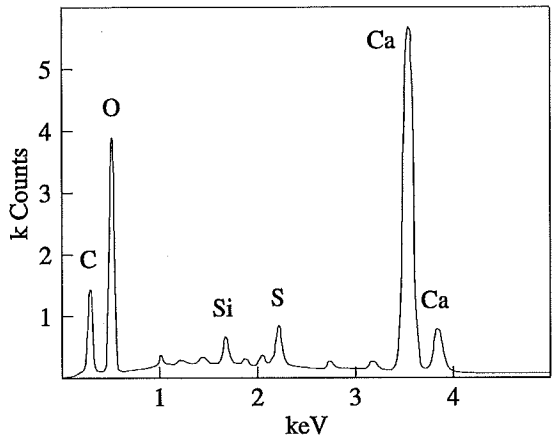

Fig. F- 5 EDS spectrum of point 4 – ettringite

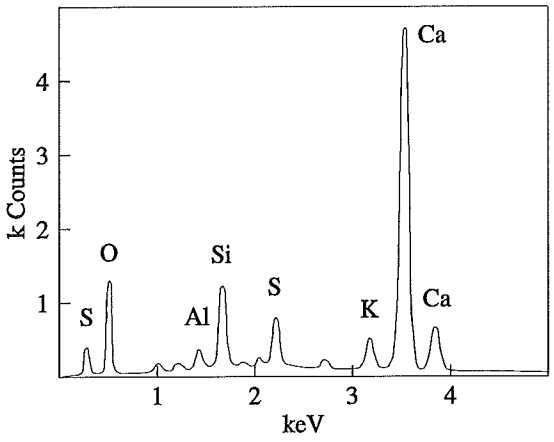

Fig. F- 6 EDS spectrum of point 5 – ettringite

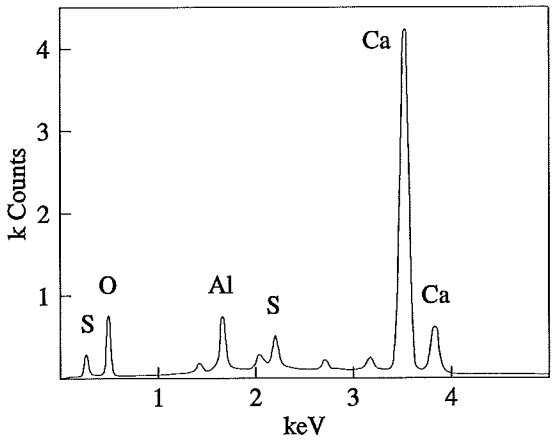

Fig. F- 7 EDS spectrum of point 6 - ettringite

APPENDIX G: SECONDARY MINERALS IN LARGE VOIDS OF MATRIX

Fig. G- 1 House 1

Fig. G- 2 House 2

Fig. G- 3 House 3

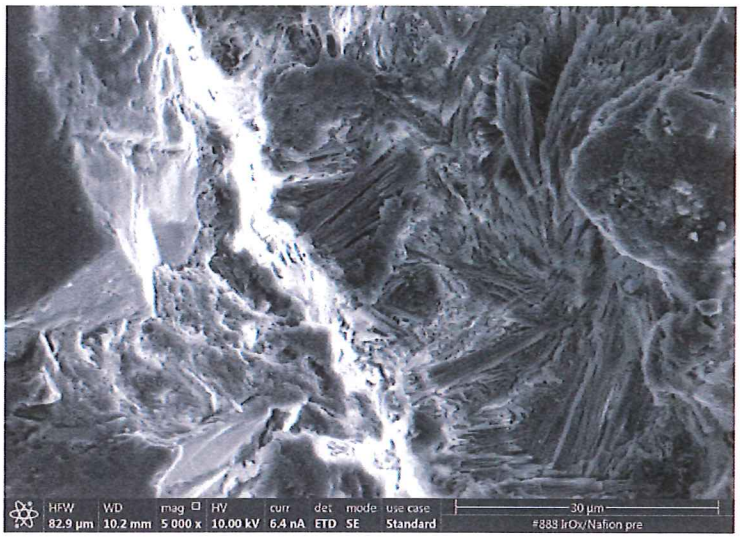

Fig. G- 4 House 4

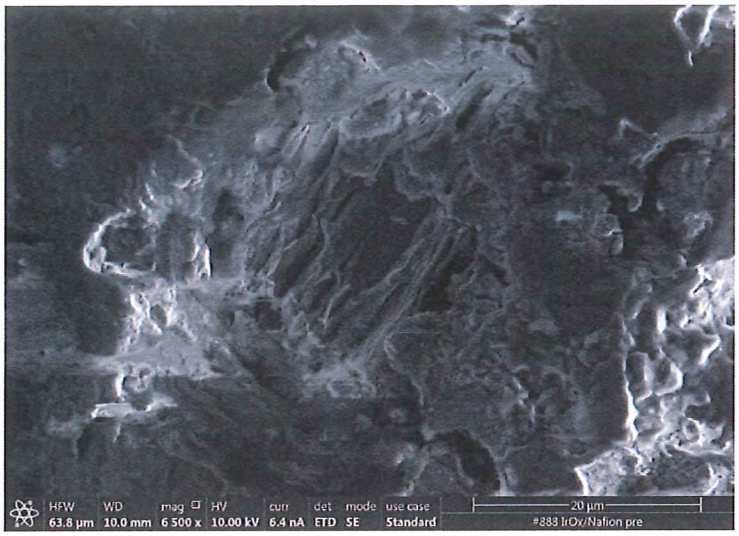

Fig. G- 5 House 5

REFERENCES

[1] Hassen, W.C., Attack on Portland cement concrete by alkali soils and waters – A critical review. *Symposium on effects of aggressive fluids on concrete* 1966.

[2] Lea, F.M., and Desch, C.H., The chemistry of cement and concrete. London, EdwardArnold and Co., 1956.

[3] Bates, P.H., Pillips, A.J., and Wig, Rudolph. Action of the salts in alkali and sea water on cements. *Journal of the Franklin Institute* 1913, 175(1): 65-67.

[4] Wig, R.J., Williams, G.M., Finn, A.N., Action of the salts in alkali and sea water on cements. *National Bureau of Standards* 1917, Tech Paper No. 95.

[5] Williams, G.M., Finn, A.N., Action of the salts in alkali and sea water on cements. *National Bureau of Standards* 1922, Tech Paper No. 214.

[6] Williams, G.M., Finn, A.N., Action of the salts in alkali and sea water on cements. *National Bureau of Standards* 1926, Tech Paper No. 307.

[7] Miller, D.G. and Manson, P.W., Laboratory and field tests of concrete exposed to the action of sulfate waters. *USDA Tech. Bull. No.* 358, 1-80, 1933.

[8] Miller, D.G. and Manson, P.W., Long-time tests of concretes and mortars exposed to sulfate waters. *Univ. of Minnesota, Agri.Exp. Sta. Tech. Bull. No.* 184, 1-107, 1951

[9] Miller, D.G., Manson, P.W. and Chen, R.T., Annotated bibliography on sulfate resistance of Portland cements, concretes and mortars. *Univ. of Minnesota Misc. Jour. Ser.*, Paper 708, 1952.

[10] Williams, G.M.., Review of investigation into the deterioration of concrete in alkali soils. *Canadian Eng.* 1922, 42: 209-210.

[11] Shelton, G.R., Action of sodium and magnesium sulfates on constituents of Portland cement. *Industrial and Engineering Chemistry* 1925, 17: 589-592.

[12] Williams, G.M., The condition of field specimens of concrete exposed to alkali soils and waters examined in December 1927. *Eng. Jour.* 1928, 184-187.

[13] Wilson, R. and Clive, A., Brief summary of tests of the effect of sulfate soils and waters on concrete. *PCA, Rept. of Dir. of Res.* 1928, 70-74.

[14] Bogue, R.H., Studies on the volume stability of Portland cement pastes. PCA Fellowship, Paper No. 55, 1-90, 1949.

[15] Lafuma, H., Theory of expansion of cements. Rev. *Mater. Constr. Trav. Publics* 1929, 243: 441-444.

[16] Nakamura, Y.G.S. and Akaiva, K., Mineralogical composition of expansive cement clinker rich in SiO_2 and its expansivity. *Proc. Int. Symp. Chem. Cem.* 1968, 4: 351-365.

[17] Bentur, A. and Ish-shalom, M., Properties of type K expansive cement of pure components: II. Proposed mechanism of ettringite formation and expansion in unrestrained paste of pure expansive components. *Cement and Concrete Research* 1974, 4: 709-721.

[18] Soroka, I., Portland cement paste and concrete. Macmillan, London 1979.

[19] Heinz, H., Ludwig, U., and Nasr, R., Model experiments to clarify damages of heat-treated mortars and concrete elements. Part II. Heat treatment of mortars delayed ettringite formation. *TIZ* 1982, 108: 178-183.

[20] Shauba W., et al., the experiments on mechanism of ettringite expansion. *Proc. Beijing Int. Symp. Cem. Concr.* 1985, 3: 43-55.

[21] Hassen, W.C., Attack on Portland cement concrete by alkali soils and waters – A critical review. *Highway Research Record* 1966, 113: 1-32.

[22] Mather, B., A discussion of the paper 'Mechanism of expansion-associated ettringite formation' by P.K. Mehta'. *Cement and Concrete Research* 1973, 3: 651-652.

[23] Hansen, W.C., A discussion of th epaper 'Scanning electron miscroscopic studies of ettringite formation' by P.K. Mehta. *Cement and Concrete Research* 1976, 6: 595-596.

[24] Tannatt, E.T. and Burke, E., Effect of alkali on Portland cement. *Montana Agri. Coll., Exp. Sta/ Bull. No.* 69, 1908.

[25] Burke, E., and Pinckney, R.M., Destruction of hydraulic cements by the action of alkali salts. *Montana Agri. Coll. Exp. Sta. Bull. No.* 81, 1910.

[26] Hansen, W.C., Solid-liquid reactions in Portland cement pastes. *Mater. Res. And Std.* 1962, 2: 490-493.

[27] Mehta, P.K., and Hu, F, further evidence for expansion of ettringite by water adsorption. *Journal of the American Ceramic Society* 1978. 61: 179-181.

[28] Mehta, P.K., Mechanism of expansion associated with ettringite formation. *Cement and Concrete Research* 1973. 3:1-6.

[29] Moor, A.E., and Taylor, H.F.W., *Nature* 1968, 218: 1048.

[30] Mehta, P.K., Mechanism of sulfate attack o Portland cement concrete – another look. *Cement and Concrete Research* 1983, 13: 401-406.

[31] Chatterji, S., Jeffery, J.W., A new hypothesis of sulfate expansion. *Magazine of Concrete Research* 1963, 15(44): 83-86.

[32] Thorvaldson, T., Chemical aspects of the durability of cement products. Proc. 3rd Int. Symp. on Chem. of Cement, London 1952, 436-466.

[33] Wolter, S., Ettringite, Cancel of Concrete, Burgess Publishing, New York, 1996.

[34] Tagnit-Hamou, A., Saric-Coric, M., Rivard, P., Internal deterioration of concrete by the oxidation of pyrrhotite aggregates. *Cement and Concrete Research* 2005, 35: 99-107.

[35] Divet, L., Activité sulfatique dans les bétons, consecutive à l'oxydation des pyrites contensus dans les aggrégats. Synthése bibliographique, Bull. Lab. Ponts Chaussées 201 (1996) 45-63.

[36] Neville, A.M., Behavior of concrete in saturated and weak solutions of magnesium sulphate or calcium chloride. *Journal Materials* 1970. 4(4): 781-816.

[37] Mehta, P.K., Mechanism of expansion associated with ettringite formation. *Cement and Concrete Research* 1973. 3: 1-6.

[38] Mehta, P.K., Hu, F., Further evidence for expansion of ettringite by water adsorption. *Journal of the American Ceramics Society* 1978. 61: 179-181.

[39] Ogawa, K., Roy, D.M., C_4A_3S hydration ettringite formation and its expansion mechanism: II. Microstructural observation of expansion. *Cement and Concrete Research* 1982. 12: 101-109.

[40] Ogawa, K., Roy, D.M., C_4A_3S hydration ettringite formation and its expansion mechanism: III. Effect of CaO, NaOH and NaCl; Conclusions. *Cement and Concrete Research* 1982. 12: 247-256.

[41] Cohen, M.D., Theories of expansion in sulfoaluminate-type expansive cements: Schools of thought. *Cement and Concrete Research* 1983. 13: 809-818.

[42] Deng, M., Tang, M., Formation and expansion of ettringite crystals. *Cement and Concrete Research* 1994. 24: 119-126.

[43] Diamond, S., Delayed ettringite formation processes and problems. *Cement and Concrete Research* 1996. 18: 205-215.

[44] Pettifier, K., Nixon, P.J., Alkali-metal sulphate a factor common to both alkali aggregate reaction and sulphate attack on concrete. *Cement and Concrete Research* 1980. 10: 173-181.

[45] Al-Amoudi, O.S.B., Abduljauwad, S.N.R., Masle-huddin, M., Effect of chloride and sulfate contamination in soils on corrosion of steel and concrete. *Transportation research record* 1992. 1345: 67-73.

[46] Pitt, J.M., Schluter, M.C., Lee, D.Y., Dubberke, W., Sulfate impurities from deicing salt and durability of Portland cement mortar. *Transportation research record* 1987. 1110: 16-23.

[47] Taylor, H.F.W., Cement Chemistry. Academic Press, London, 1990.

[48] Robie, Hemingway, B.S., Fisher, J.R., U.S. *Geological Survey Bulletin No. 1452*, 1978.

[49] Casanova, I., Agulló, L., and Aguado, A., Aggregate expansivity due to sulfide oxidation I. reaction system and rate model. *Cement and Concrete Research* 1996. 26(7): 993-998.

[50] Chinchón, J.S., Ayora, C., Aguado, A., Guirado, F., Influence of weathering of iron sulfides contained in aggregates on concrete durability. *Cement and Concrete Research* 1995. 25(6): 1264-1272.

[51] Thomas, M.D.A., Kettle, R.J., Morton, J.A., The oxidation of pyrite in cement stabilized colliery shale. *Quarterly Journal of Engineering Geology & Hydrogeology* 1989. 22(3): 207-218.

[52] Shayan, A., Deterioration of a concrete surface due to the oxidation of pyrite contained in pyritic aggregate. *Cement and Concrete Research* 1988. 18: 723-730.

[53] Ayora, C., Chinchón, S., Aguado, A., Guirado, F., Weathering of iron sulfide and concrete alteration: Thermodynamic model and observation in dams from central Pyrenees Spain, *Cement and Concrete Research* 1998. 28(9): 1223-1235.

[54] Moum, J., Rosenqvist, I.T., Sulfate attack on concrete in the Oslo region. *Journal of American Concrete Institute* 1959. 56(9): 257-264.

[55] Quigley, R.M., Vogan, R.W., Black shale heaving at Ottawa, Canada. *Canadian Geotechnical Journal* 1970. 7(2): 106-112.

[56] Bérard, J., Black shale heaving at Ottawa, Canada: Discussion. *Canadian Geotechnical Journal* 1970. 7(2): 113-114.

[57] Bérubé, M.A., Locat, J., Gélinas, P., Chagon, J.Y., and Lefrancois, P., Heaving of black shale in Québec City. *Canadian Journal of Earth Sciences* 1986. 23: 1774-1781.

[58] Côté, F., Expansion de shales pyriteux. M.Sc. thesis, Département de genie mineral, École Polytechnique de Montréal, Montréal,Qué, 1990.

[59] Côté, F., Bérard, J., Roux, R. Cas de réactivité et de gonflement de remblais granulaires riches en shale pyriteux. *Collection Environment et Géologie, APGGQ* 1991. 12: 225-246.

[60] Duchesne, J., Benoît, F., Deterioration of concrete by the oxidation of sulphide minerals in the aggregate. *Journal of Civil Engineering and Architecture* 2013. 7(8): 922-931.

[61] Rodrigues, A., Duchesne, J., Fournier, B., Durand, B., Rivard, P., Shehata, M., Mineralogical and chemical assessment of concrete damaged by the oxidation of sulfide-bearing aggregates: Importance of thaumasite formation on reaction mechanisms. *Cement and Concrete Research* 2012. 42: 1336-1347.

[62] Lee, H., Cody, R.D., Cody, A.M., Spry, P.G., The formation and role of ettringite in Iowa highway concrete deterioration. *Cement and Concrete Research* 2005. 35: 332-343.

[63] Oliveira, I., Cavalaro, S.H.P., Aguado, A., Evolution of pyrrhotite oxidation in aggregates for concrete. *Materials de Construcción* 2014. 64(316).